Extent to which international wind turbine design standard, IEC61400-2 is valid for a rooftop wind installation

Amir Bashirzadeh Tabrizi[*a], Jonathan Whale[a], Thomas Lyons[b], Tania Urmee[a]

[a] *Physics and Energy Studies, School of Engineering and Information Technology, Murdoch University, Perth, WA 6150, Australia*

[b] *Environmental Science, School of Veterinary and Life Sciences, Murdoch University, Perth, WA 6150, Australia*

Abstract

The use of small grid-connected wind turbines is increasing within the built environment, yet atmospheric turbulence in this environment is more complex than the open terrain sites on which the turbine design standards are based. The current IEC61400-2 design standard uses stochastic turbulence models adapted from the von Karman and Kaimal power spectra in order to simulate flow fields that are used by designers to predict structural loading on small wind turbines. Both spectra are based on observations in the atmospheric surface layer developed over flat, smooth and uniform terrain yet IEC61400-2 does not offer any modifications of the spectra for more complex terrain such as that which exists in the built environment. This paper investigates the extent to which the von Karman and Kaimal models, as presented in IEC61400-2, are appropriate for use in the design of SWTs installed on the rooftop of a warehouse in the built environment. In particular the paper attempts to gauge how different the turbulence spectra currently used for turbine design are from the actual inflow conditions experienced by the turbines on the roof.

The power spectra of all three wind components in neutral and slightly unstable atmospheric conditions at four heights above the rooftop are considered. A degree of misfit function was used to compare von Karman, Kaimal and measured power spectra, as an indicator of model suitability. A sensitivity study was carried out to assess the influence of turbulence length scale and wind direction on the results. The Kaimal spectral function was the better of the existing models in predicting the trends of all wind components and was used as a starting point in developing an approach to modelling turbulence power spectra for a rooftop site in the built environment by incorporating typical length scales at the site.

Keywords: Small wind turbines, Built environment, Rooftop site, Power spectral density, IEC61400-2

Nomenclature

a	Slope parameter for characteristic turbulence standard deviation model [-]
d_{misfit}	Degree of misfit [-]

[*] Corresponding author. Tel.: +61893606713; e-mail: a.btabrizi@murdoch.edu.au. ; address: School of Engineering and Information Technology, Murdoch University, 90 South Street, Murdoch, WA 6150, Australia.

f	Frequency [Hz]
g	Gravitational acceleration constant [m/s^2]
h	Façade height of the Bunings warehouse roof a.g.l [m]
I_{15}	Characteristic value of hub-height turbulence intensity at a 10-minute average wind speed of 15 m/s [-]
k	Index for the velocity component direction (i.e. 1 = longitudinal, 2 =lateral, and 3 = vertical) [-]
L	Monin-Obukhov length scale [m]
l	The velocity component integral scale parameter [m]
P_R	Cumulative wind speed probability distribution [-]
$S_1(f)$	Power spectral density of the longitudinal component of turbulence [(m/s)^2/Hz]
S_k	Single-sided velocity component spectrum [(m/s)^2/Hz]
$\overline{T_0}$	Mean air temperature [K]
u_*	Friction velocity [m/s]
$\vec{U}$	Wind velocity vector [m/s]
$\vec{\overline{U}}$	Mean wind velocity vector [m/s]
$\vec{u}$	Fluctuation in wind velocity [m/s]
u_s	Longitudinal wind speed from the ultrasonic (raw data) [m/s]
u_{2d}	Longitudinal component of the horizontal wind speed [m/s]
u_{3d}	Longitudinal component of the three-dimensional wind speed (reference frame of the mean three-dimensional wind speed) [m/s]
V_{hub}	Mean horizontal wind speed at the hub-height of the turbine [m/s]
V_{ave}	Annual average horizontal wind speed at hub height [m/s]
V(z)	Horizontal wind speed at height z [m/s]
v_s	Lateral wind speed from the ultrasonic (raw data) [m/s]

v_{3d}	Lateral component of the three-dimensional wind speed (reference frame of the mean three-dimensional wind speed) [m/s]
$\overline{\acute{w}\acute{T}}$	Kinematic heat flux [mK/s]
w_s	Vertical wind speed from the ultrasonic (raw data) [m/s]
w_{3d}	Vertical component of the three-dimensional wind speed (reference frame of the mean three-dimensional wind speed) [m/s]
z	Height a.g.l. [m]
z_{hub}	Height of the turbine hub a.g.l. [m]
$\acute{z_s}$	Effective height [m]
κ	von Karman's constant [-]
α	Wind shear power law exponent [-]
$\Lambda 1$	Turbulence scale parameter [m]
σ_1	Hub-height longitudinal wind velocity standard deviation [m/s]
σ_k	Standard deviation of the velocity component [m/s]
σ_x	Standard deviation of x [m^2/s^2]
$\sigma_{u_s v_s}$	Covariance between u_s and v_s [m^2/s^2]
$\sigma_{u_{2d} w_s}$	Covariance between u_{2d} and w_s [m^2/s^2]
θ	Wind direction in the horizontal plane [degree]
φ	Flow direction at an incline to the horizontal [degree]

1. Introduction

Small wind turbines (SWTs), defined as having a swept area less than 200 m^2, have traditionally been used in off-grid areas in open terrain exposed to the wind. There has, however, been an increasing trend towards the installation of SWTs in non-open terrain, such as the built environment, above forests and in mountainous areas [1].The drivers for this change in turbine location include the expansion of the small wind market into new areas of the globe, and the increased use of grid-connected SWT by businesses and homes in urban areas as part of a reaction to high electricity prices and a desire to be energy independent. In terms of use in the built environment there has been increased interest among architects,

project developers and local governments in using SWTs as part of sustainable and low-energy buildings [2].

There have, however, been some notable failures of small wind turbines in the built environment, particularly where turbines were mounted on top of buildings [e.g. 3,4]. There is some evidence that these failures are linked to inadequate turbine design for the resource at the site. Many of these complex terrain sites are often characterised by highly turbulent wind flow, and elevated turbulence intensity has been found to be the most important factor in reducing turbine fatigue life [5]. The current IEC international design standard for SWTs, IEC61400-2, is based on wind turbines in open terrain and does not include specific design models for highly turbulent sites [2]. In particular built environment sites include locations near buildings, trees and other obstacles, and in such locations, the wind is normally highly three-dimensional, turbulent, unstable and weak, in terms of direction and speed [5], and some sites may experience values of inflow turbulence intensity that are many times greater than an open field site. The research question then arises as to what extent the existing turbulence models used in IEC61400-2 are suitable for use in highly turbulent sites.

There is a considerable body of literature that provides a framework for the description of the turbulence structure in the atmospheric boundary layer over open terrain and the description of the properties of atmospheric turbulence is becoming more complete and more reliable through improved sensors and data programs [6]. Detailed measurements of turbulence over open terrain under different conditions of atmospheric stability show that current theories describe the flow over these surfaces quite well [7, 8]. Measurements over uniform terrain, including cases exhibiting roughness changes in the upwind direction, were reviewed by ESDU to investigate the atmospheric turbulence characteristics near the ground and calculate the turbulent integral length scales [9]. Shiau and Chen conducted on-site observations and measured the wind characteristics and velocity spectra near the ground at the northeastern coast of Taiwan. Their results showed that the properly scaled spectrum of longitudinal wind velocity was in good agreement with von Karman's power spectrum equation. They also showed that properly scaled measurements of the lateral and vertical wind velocity spectra were close to the results of the isotropic turbulence spectra equations [10]. For flow over complex terrain, where the turbulent flow structure is affected by topographic variations, agreement is less clear [6]. Within the built environment, for instance, less is known of the properties of atmospheric turbulence. Although Tieleman [11], for example, has developed expressions for spectra above perturbed terrain, and these expressions can be useful for describing the flow well above the direct influence of local obstacles, they are not suitable at heights close to the obstacles.

In IEC61400-2, the existing international standard for small wind turbines, the von Karman and Kaimal spectral density functions have both been suggested for use in stochastic turbulence models that can be used for turbine design load calculations. Despite being used for turbines that are later installed in the built environment there is no indication within the standard of the accuracy of these models for such an environment [12]. Indeed, the von Karman spectrum was derived for isotropic turbulence, behind a grid, and later applied with adjustments, to atmospheric turbulent flow. The Kaimal spectrum was derived from meteorological measurements. Both models are based on observations in the atmospheric surface layer developed over flat, smooth and uniform terrain. It is evident that these models do not represent the observations over terrain with upwind roughness elements or upwind topographic features (complex terrain).

In this work, we investigate the extent to which the von Karman and Kaimal models, as presented in IEC61400-2, are appropriate for the case of five SWTs installed on the rooftop of a warehouse in the built environment and attempt to gauge how different the turbulence spectra used for turbine design are from the actual inflow conditions experienced by the turbines.

The turbulence power spectral densities of the three components of wind speed are measured on the rooftop of the Bunning Group Ltd's warehouse at Port Kennedy in Western Australia, under different atmospheric conditions. Measurements are compared with calculated spectral densities from the von Karman and Kaimal models to assess the suitability of these models for predicting the structure of the turbulence at a SWT site in the built environment. The investigation was performed at four different heights above the rooftop of the warehouse. At each height the power spectral densities for the three wind components at the two atmospheric conditions were calculated from direct measurement and compared with the corresponding von Karman and Kaimal spectral models as defined in IEC61400-2. A misfit function was used to quantify discrepancies between the measurements and the model predictions. The scope of this paper includes suggesting an approach to adapt one of the existing turbulence models in the IEC61400-2 standard for use in the built environment by providing a correction based on estimation of suitable integral length scale values. The research has links with the current International Energy Agency (IEA) Task 27 program of work that aims to develop a Recommended Practice for micro-siting SWTs in the built environment [13].

2. Theory

2.1. Turbulence and Thermal Stability

Turbulence is affected by atmospheric thermal stability conditions, which depend on the potential temperature gradient. The turbulent eddies in an unstable boundary layer can extend vertically for a significant distance. In neutral, or near-neutral atmospheric conditions, the air is well-mixed and the vertical potential temperature gradient is close to zero, resulting in buoyancy forces that are negligible. High wind speeds and cloudy skies prevent any significant temperature gradient forming and lead to neutral atmospheric conditions [14].

The cut-in wind speed for most SWTs that are appropriate for rooftop applications is, at a minimum, 2 m/s and most of the power generated by a turbine on the roof occurs at wind speeds greater than 4 m/s. For most operational states of small rooftop wind turbines the atmospheric conditions are either slightly unstable or neutral [15].

The boundary layer can be stratified according to the parameter known as the Monin Obukhov length, *L*; which is the height where the turbulent forcing from thermal and shear processes are in balance. *L* is constant with height but changes with stability in the surface layer and as a result can be used as a measure of stability [16]. *L* is defined as:

$$L = \frac{-u_*^3 \overline{T_0}}{g\kappa \overline{\acute{w}\acute{T}}} \qquad (1)$$

Golder [17], using micro-meteorological data, presented curves linking Pasquill's stability classes to *L* and the roughness length, z_0.

2.2. Turbulent Power Spectral Density

A three-dimensional wind velocity vector $\vec{U}$ can be defined as:

$$\vec{U} = \vec{\bar{U}} + \vec{U} \qquad (2)$$

where $\vec{\bar{U}}$ is the mean wind velocity vector and $\vec{U}$ is the fluctuation about the mean wind. Power spectral densities are often used in wind turbine rotor dynamics to look at the dynamic loads on the blades. There are a number of power spectral density functions that are applied as models in wind energy engineering when, for a given site, representative turbulence power spectral densities are unavailable [18].

In the IEC61400-2 standard [12], the von Karman and Kaimal spectral density functions have been suggested as stochastic turbulence models that can be used for design load calculations. In the standard, a random vector field has been considered for the turbulent velocity fluctuations where the components of wind fluctuations have zero-mean Gaussian statistics. The power spectral densities of the wind velocity components are presented in terms of either the Kaimal turbulence model or the von Karman isotropic turbulence model.

These models have been adapted to simulating inflow into the turbine rotor by satisfying the following:

1. The cumulative probability distribution at hub height is given by:

$$P_R(V_{hub}) = 1 - \exp\left[-\pi(V_{hub} / 2V_{ave})^2\right] \qquad (3)$$

2. The wind shear profile is assumed to be given by a power law with exponent of 0.2:

$$V(z) = V_{hub}(z / z_{hub})^{\alpha} \qquad (4)$$

3. The characteristic value of the standard deviation of longitudinal wind velocity is given by:

$$\sigma_1 = I_{15}(15 + aV_{hub})/(a+1) \qquad (5)$$

4. Towards the high frequency end of the inertial subrange the power spectral density of the longitudinal component of the turbulence asymptotically approaches:

$$S_1(f) = 0.05(\sigma_1)^2(\Lambda_1 / V_{hub})^{-2/3} f^{-5/3}$$

where the turbulence scale parameter is given by:

$$\Lambda_1 = \begin{cases} 0{,}7z_{hub} & \text{for } z_{hub} < 30\text{m} \\ 21\text{m} & \text{for } z_{hub} \geq 30\text{m} \end{cases} \qquad (6)$$

2.2.1 Kaimal spectral model

In the standard [12], the component power spectral densities are addressed in non-dimensional form by the following equation:

$$\frac{fS_k(f)}{\sigma_k^2} = \frac{4fl/V_{hub}}{(1+6fl/V_{hub})^{5/3}} \quad (7)$$

where

$$\sigma_k^2 = \int_0^\infty S_k(f)df \quad (8)$$

The turbulence spectral parameters suggested in the standard are listed in Table 1.

Table 1
Turbulence spectral parameters for Kaimal model [12]

	Velocity component index(k)		
	1	2	3
Standard deviation σ_k	σ_1	$0.8\sigma_1$	$0.5\sigma_1$
Integral scale, l_k	$8.1\Lambda_1$	$2.7\Lambda_1$	$0.66\Lambda_1$

where, for wind turbines of hub-height less than 30 m (typical of SWTs), the scale of turbulence Λ_1 is assumed to be 70% of turbine hub-height.

2.2.2 von Karman isotropic turbulence model

The longitudinal velocity component spectrum is given in the standard [12] by the non-dimensional equation :

$$\frac{fS_1(f)}{\sigma_1^2} = \frac{4fl/V_{hub}}{(1+71.(fl/V_{hub})^2)^{5/6}} \quad (9)$$

where the integral scale parameter, *l*, is 3.5 times the scale of turbulence Λ_1 (again taken to be 70% of turbine hub-height).

Since the model assumes isotropic turbulence, the lateral and vertical spectra are assumed equal and presented in non-dimensional form as:

$$\frac{fS_2(f)}{\sigma_2^2} = \frac{fS_3(f)}{\sigma_3^2} = 2f\,l/V_{hub} \cdot \frac{1+189.(fl/V_{hub})^2}{(1+71.(fl/V_{hub})^2)^{11/6}} \quad (10)$$

where l is the same isotropic scale parameter used in equation (9).

The fundamental concept of the isotropic turbulence model is that the statistical properties of turbulence are independent of direction. Whilst horizontal isotropy is feasible over an infinite plain site [19], it is clearly not achievable over a heterogeneous built environment.

2.3. Misfit function

Maus and Dimri [20] use a misfit function to quantify how well model spectra fit to measured data. In their work, the distance between the measured power spectrum and model power spectrum at each wave number is quantified using a norm given by the absolute difference between the logarithms of the measurement and model values. Integration of the norm over the whole spectrum produces the degree of misfit, where the smaller the integral value, the better the fit:

$$d_{misfit} = \int_0^\infty |\log(S_{\text{measured}}) - \log(S_{model})|\, df \qquad (11)$$

To give some insight into the degree of misfit function, if the model overestimates or underestimates the measured values by a factor of 5 across the range of the spectra, the degree of misfit will be 5.75. On the other hand if there is only a 5% difference between the model values and the measurements across the spectral range, the degree of misfit will be 0.17. In this research, the degree of misfit has been used to quantify the distance between the von Karman and Kaimal spectral models and the measured power spectra of winds over the rooftop for all three components of wind velocity.

3. Method

3.1 Site and Measurements

This study makes use of data collected from a wind monitoring system on the roof of a large warehouse belonging to the hardware chain Bunnings Ltd. in the suburb of Port Kennedy, Perth, Western Australia. The warehouse is a rectangular building of height h = 8.5 m a.g.l, with its long-axis oriented NNE-SSW, and a very low pitched roof (almost flat) with a façade wall around the edge. The building lies approximately 5 km from the coast (Indian Ocean) with the prevailing winds from the south-west. The warehouse is situated in a commercial estate but has no larger buildings or large trees in the vicinity. Within a 1 km radius of the site there are mainly residential buildings to the north, commercial and industrial buildings to the east and a few buildings, low shrubs and low sand dunes to the south and west. The south-west front and the north-west side are comparatively open, though street furniture[1] and a car park exist on these sides [21]. The built-up area surrounding the warehouse is shown in Figure 1.

[1] Objects and pieces of equipment installed on streets and roads for various purposes

The wind monitoring system was installed in September 2009 as part of a wind resource assessment for the installation of five small wind turbines that were later commissioned in March 2010. A Gill WindMaster Pro 3D ultrasonic anemometer was installed on a boom on a 5.3 m mast attached to the front-façade in the south west corner of the warehouse. The boom had a sliding collar in order to position the ultrasonic anemometer at different heights above the roof. The mast could be tilted down in order to make adjustments or to replace sensors. The data consists of 10Hz data over almost 1 year period from March 2011 to February 2012. To reduce processing time, smaller records of 10 days of data were extracted for each of 4 normalized heights studied; z/h = 1.35, 1.46, 1.58 and 1.70, where z is the height of the anemometer a.g.l. The chosen positions for ultrasonic measurements are in the range of typical heights and situations that SWTs have previously been installed on rooftops. Despite the increased turbulence near the edge of the roof compared to the middle of the roof, it is not uncommon for SWTs to be installed close to the edge of the roof to ensure ease of access for maintenance. In addition the location of the turbines and anemometer mast on the front façade of the building offered Bunnings maximum publicity from the project. Further, to reduce tower installation costs and comply with local government planning regulations, SWTs are usually installed close to the rooftop on short towers with a typical upper range of around 5m. Figures 2a to 2c show the position of the ultrasonic anemometer on the roof of the Bunnings warehouse with regards to the installed SWTs.

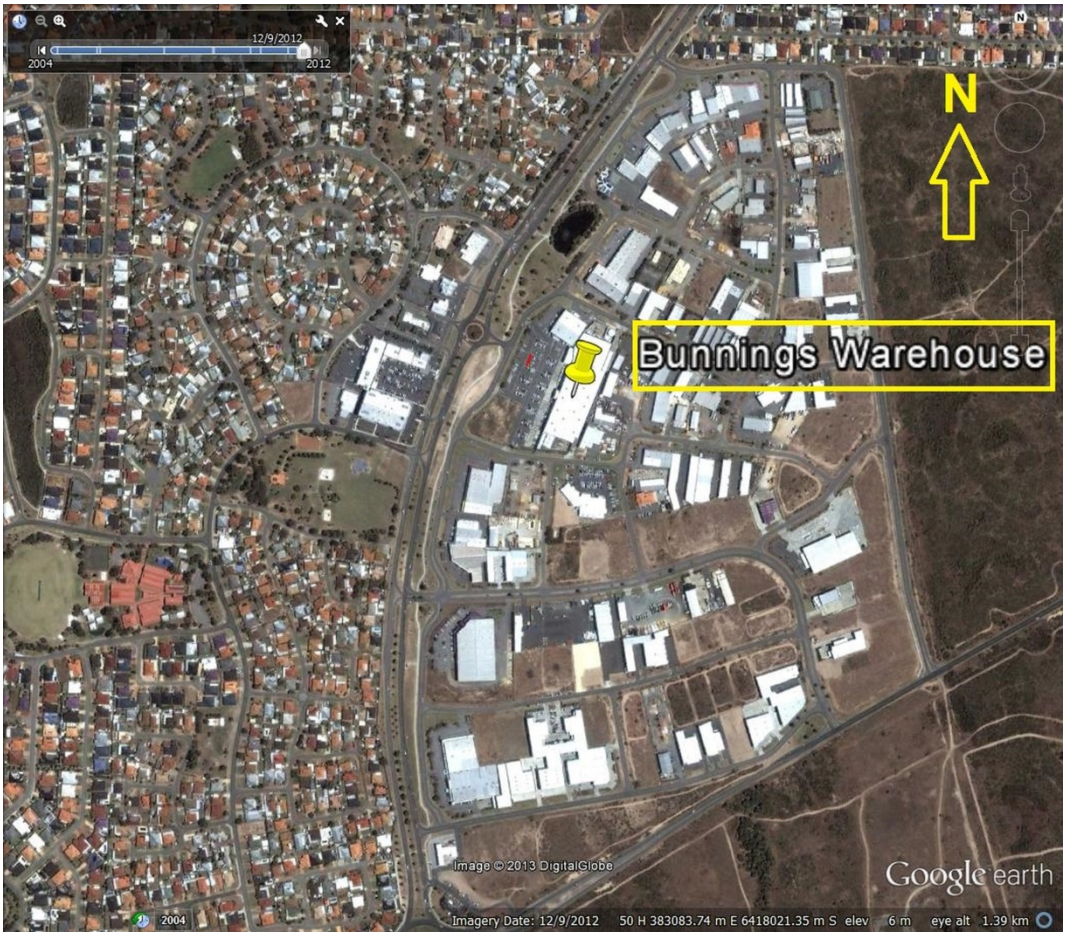

Figure1. Aerial view of the built-up area surrounding the Bunnings warehouse in Port Kennedy, WA.

Figure 2a. A photograph of the front view of the Bunnings warehouse showing the five small wind turbines and the ultrasonic anemometer position (red circle).

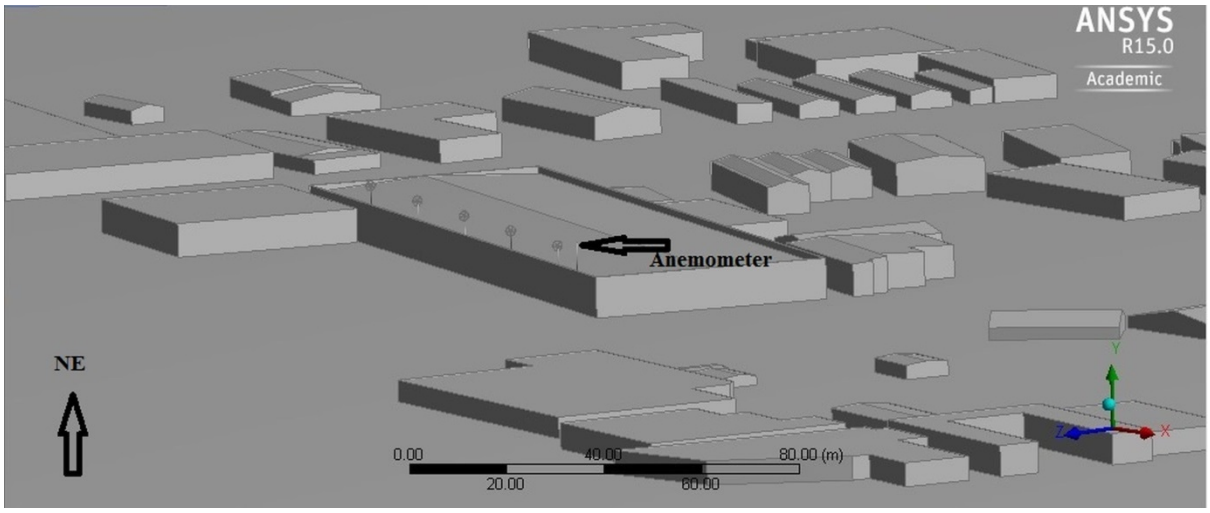

Figure 2b. Anemometer location on the rooftop of the Bunnings warehouse Building

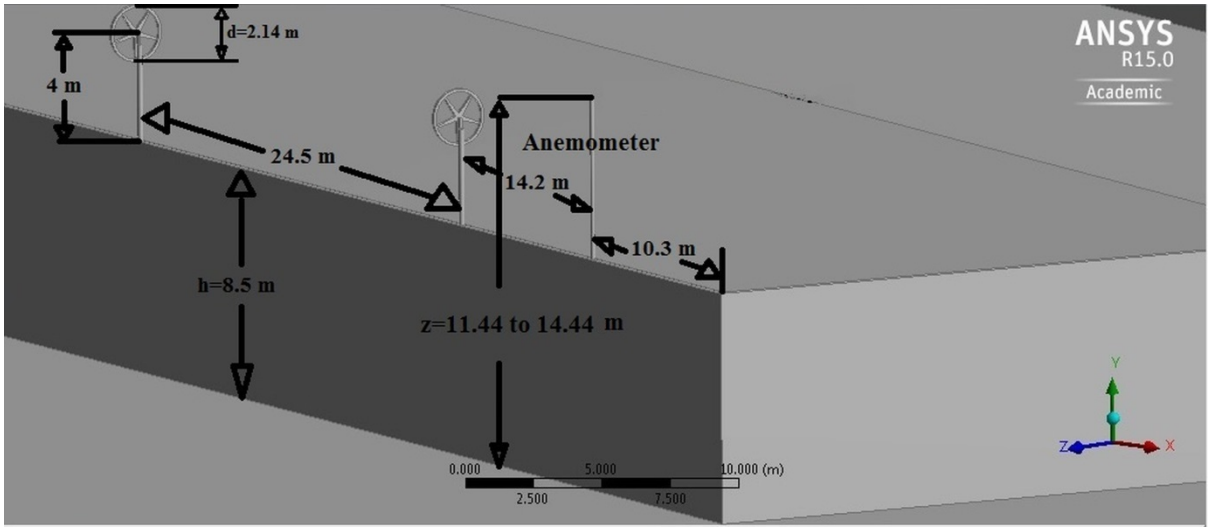

Figure 2c. Close view of anemometer location on the rooftop of the Bunnings warehouse Building

3.2. Data Analysis

Each data series, consisting of 10 days' worth of 10-minute averaged records of wind data at a known height from the rooftop of the warehouse, was analysed to investigate the suitability of the turbulence models from the design standard for use at this site.

As stated in Section 2, the most common atmospheric conditions experienced during the operation of an SWT in the built environment are either slightly unstable or neutral conditions. Thus the first step in processing the data was to filter each component of the raw three-dimensional wind speed measurements (longitudinal, lateral and vertical) using Pasquill stability classes in order to select only wind data recorded under slightly unstable or neutral conditions. Based on a table of roughness lengths, surface characteristics and roughness classes from the European wind atlas [22], the aerodynamic roughness of the Bunnings warehouse area was estimated to be 50 cm. The displacement height of the area, based on the equation presented by Panofsky & Dutton [23], has been calculated as 4.1 m. The curves presented by Golder [17], were then used to find the range of Monin-Obukhov lengths corresponding to slightly unstable and neutral conditions on the roof of the and these values were then used to filter the raw measurements.

The next part of the procedure was to rotate the filtered wind speed data from the reference frame of the ultrasonic anemometer to the reference frame of the mean three-dimensional wind speed (longitudinal, lateral and vertical) and direction, for each 10-minute averaged record. This was a two step process. Firstly, the filtered data for each dataset was binned and averaged with respect to 10 minutes time intervals, allowing standard deviations of wind speed data for each bin to be calculated. From the time-averaged data the wind direction in the horizontal plane, θ, was computed along with the covariance $\sigma_{u_S v_S}$. These parameters were used to rotate the data from the reference frame of the ultrasonic anemometer to the reference frame of the horizontal wind speed and direction, in accordance with:

$$\sigma_{u_{2d}}^2 = \sigma_{u_s}^2 \,.\cos^2\theta + \sigma_{v_s}^2 \sin^2\theta - 2\sin\theta\cos\theta\,.\,\sigma_{u_s v_s} \quad (12)$$

$$\sigma_{v_{2d}}^2 = \sigma_{v_{3d}}^2 = \sigma_{u_s}^2 \,.\sin^2\theta + \sigma_{v_s}^2\,.\cos^2\theta + 2\sin\theta\cos\theta\,.\,\sigma_{u_s v_s} \quad (13)$$

Figure 3a shows the first rotation of reference frame. In the next step, the averages and standard deviations of u_{2d} and w_s in each bin were calculated. From the time-averaged data the direction of flow at an incline to the horizontal, φ, was computed along with the covariance $\sigma_{u_{2d}w_s}$. Similar to the first step, these parameters were used to rotate the data from the reference frame of the horizontal wind speed to the reference frame of the mean three-dimensional wind speed and direction, in accordance with:

$$\sigma_{u_{3d}}^2 = \sigma_{u_{2d}}^2 \,.\cos^2\varphi + \sigma_{w_s}^2 \sin^2\varphi + 2\sin\varphi\cos\varphi\,.\,\sigma_{u_{2d}w_s} \quad (14)$$

$$\sigma_{w_{3d}}^2 = \sigma_{u_{2d}}^2 \,.\sin^2\varphi + \sigma_{w_s}^2\,.\cos^2\varphi - 2\sin\varphi\cos\varphi\,.\,\sigma_{u_{2d}w_s} \quad (15)$$

Figure 3b shows the second rotation of reference frame.

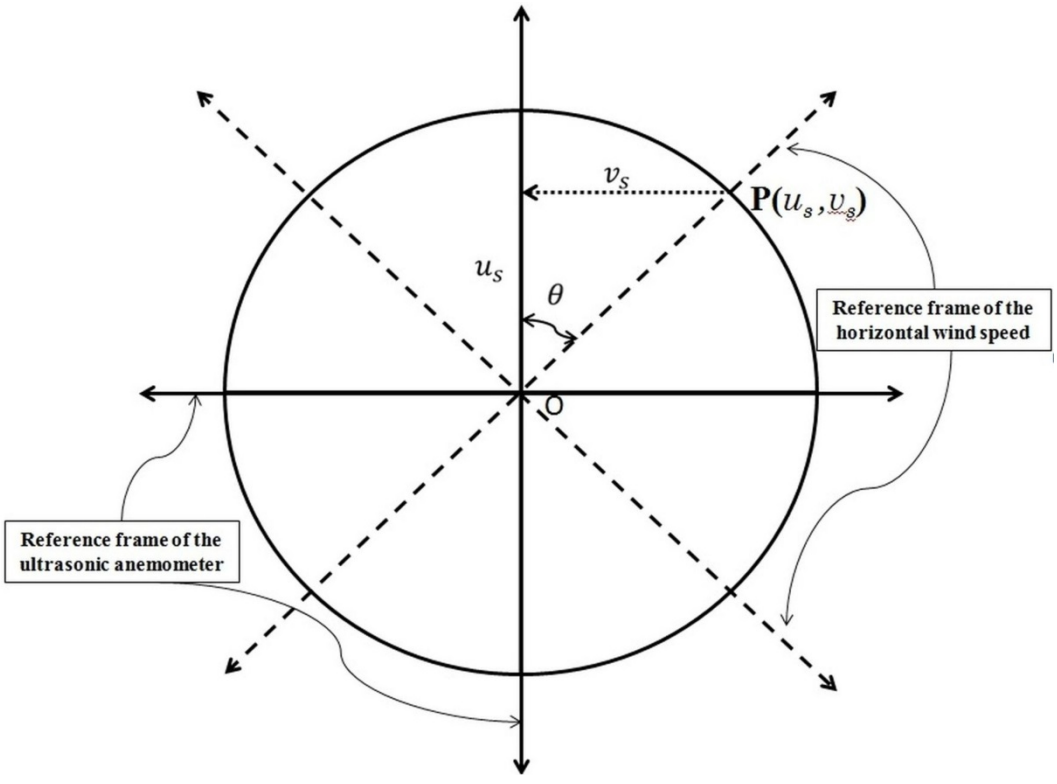

Figure3a. Changing the reference frame of the ultrasonic anemometer to the reference frame of the horizontal wind speed and direction.

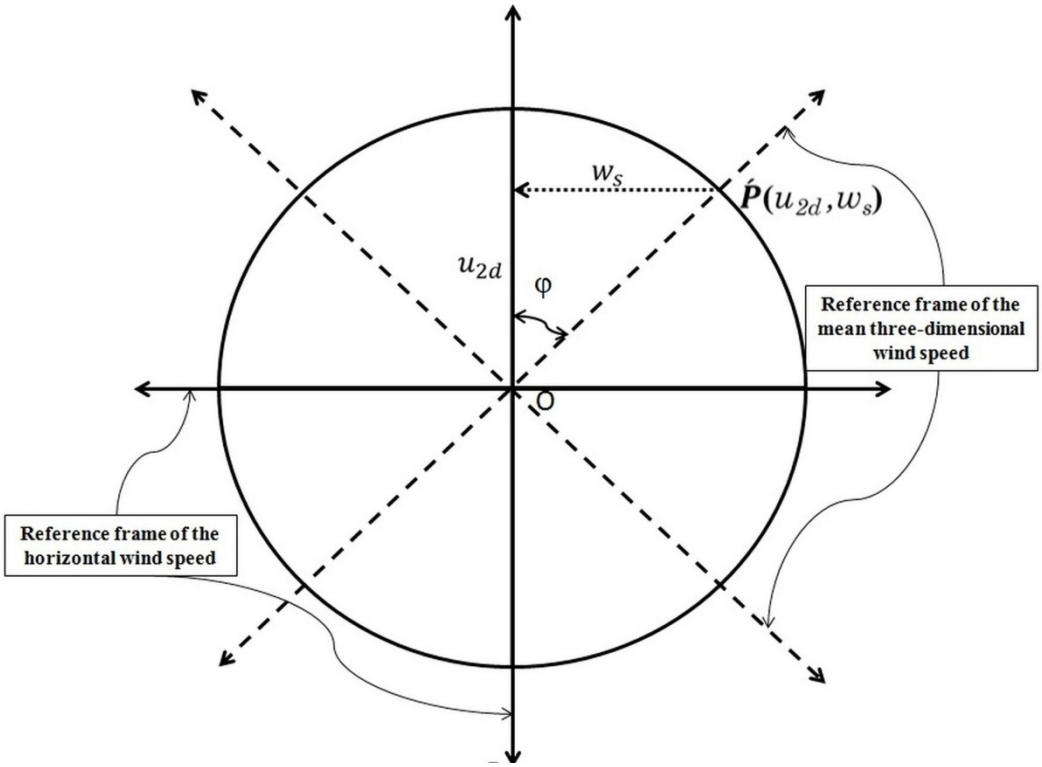

Figure3b. Changing the reference frame of the horizontal wind speed to reference frame of the mean three-dimensional wind speed and direction.

To find the turbulence power spectral density data for each 10-minute averaged record the mean longitudinal, lateral and vertical wind components were separately subtracted from their respective measurements to leave the fluctuations for each component. The autocorrelation of the fluctuations was then computed and a Fast Fourier Transform of this autocorrelation provided the data for the power spectral density plots.

The power spectra for different ten-minutes records at *z/h* = 1.35, 1.46, 1.58 and 1.70 in neutral and slightly unstable atmospheric conditions for longitudinal, lateral and vertical components were calculated, averaged over the 10 day period and compared with predictions from the von Karman and Kaimal spectra models.

4. Results and Discussion

Figure 4(a-c) shows the average values of turbulence power spectral density, S_k, for longitudinal (k = 1), lateral (k = 2) and vertical (k = 3) wind components plotted against normalized frequency ($f\acute{z_s}/U, \acute{z_s} = z - z_d$) for neutral atmospheric conditions. Figure 5(a-c) shows the equivalent plots for slightly unstable atmospheric conditions. Predicted values by the von Karman and Kaimal models are shown for comparison in each plot.

The plots for neutral atmospheric conditions at *z/h* = 1.35, 1.46, 1.58 and 1.70 were the result of averaging 390, 243, 570 and 514 ten-minute recordings, respectively, whereas the plots for slightly unstable atmospheric conditions at *z/h* = 1.35, 1.46, 1.58 and 1.70 were achieved by averaging 355, 277, 353 and 333 ten-minute recordings, respectively.

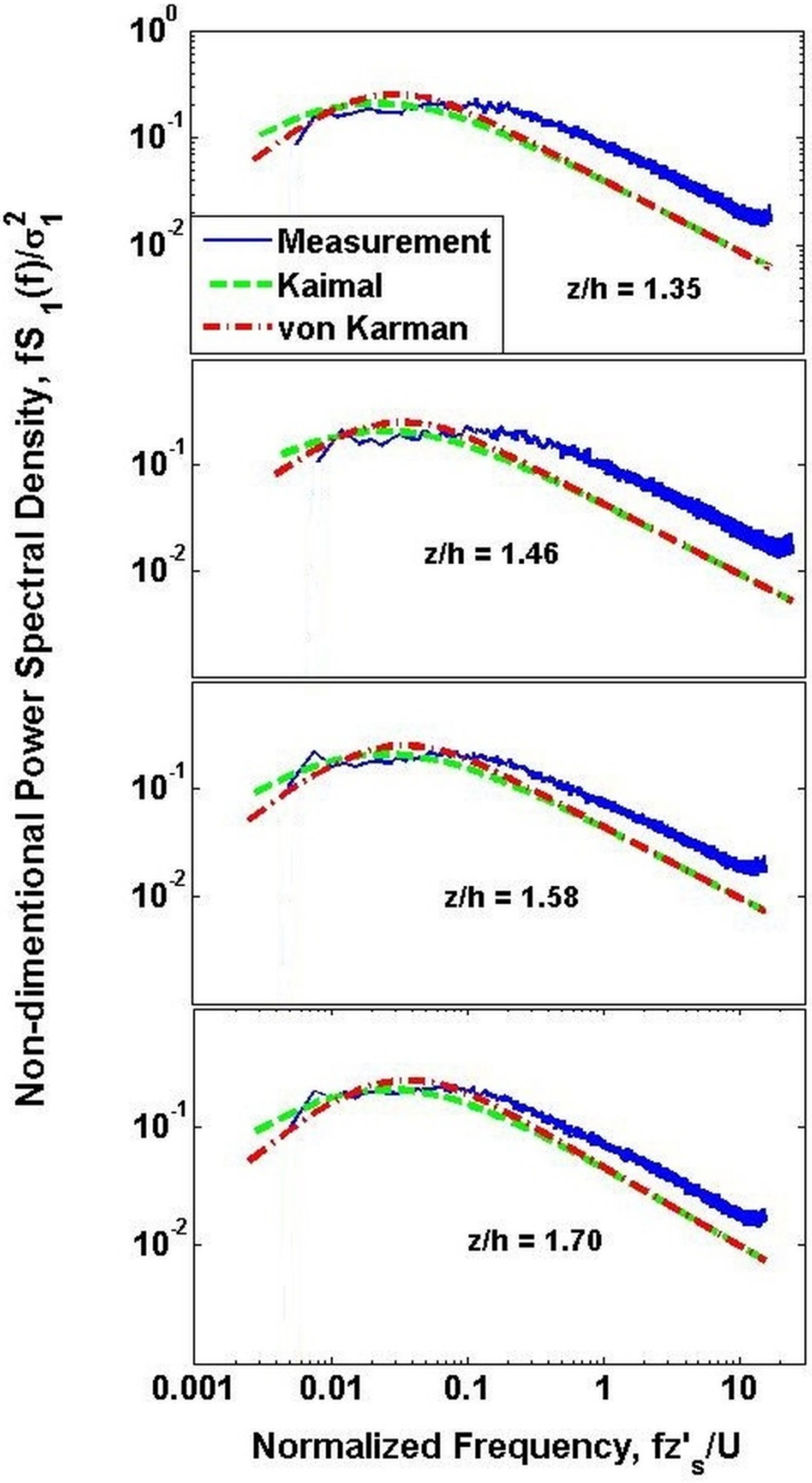

Figure 4a.Non-dimensional turbulence power spectral density of the **longitudinal** wind speed component for different heights above the rooftop of a warehouse in neutral atmospheric conditions.

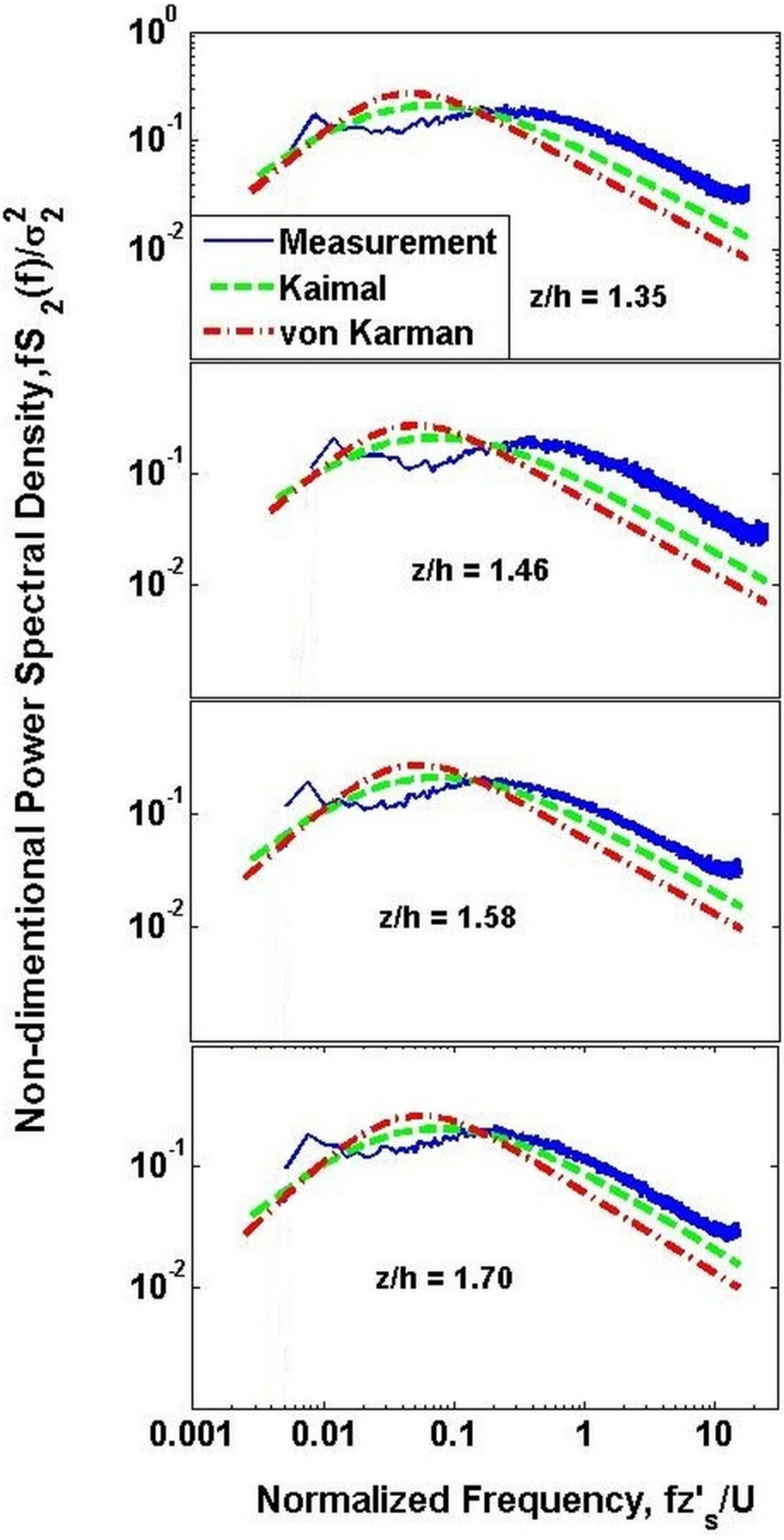

Figure 4b. Non-dimensional turbulence power spectral density of the **lateral** wind speed component for different heights above the rooftop of a warehouse in neutral atmospheric conditions.

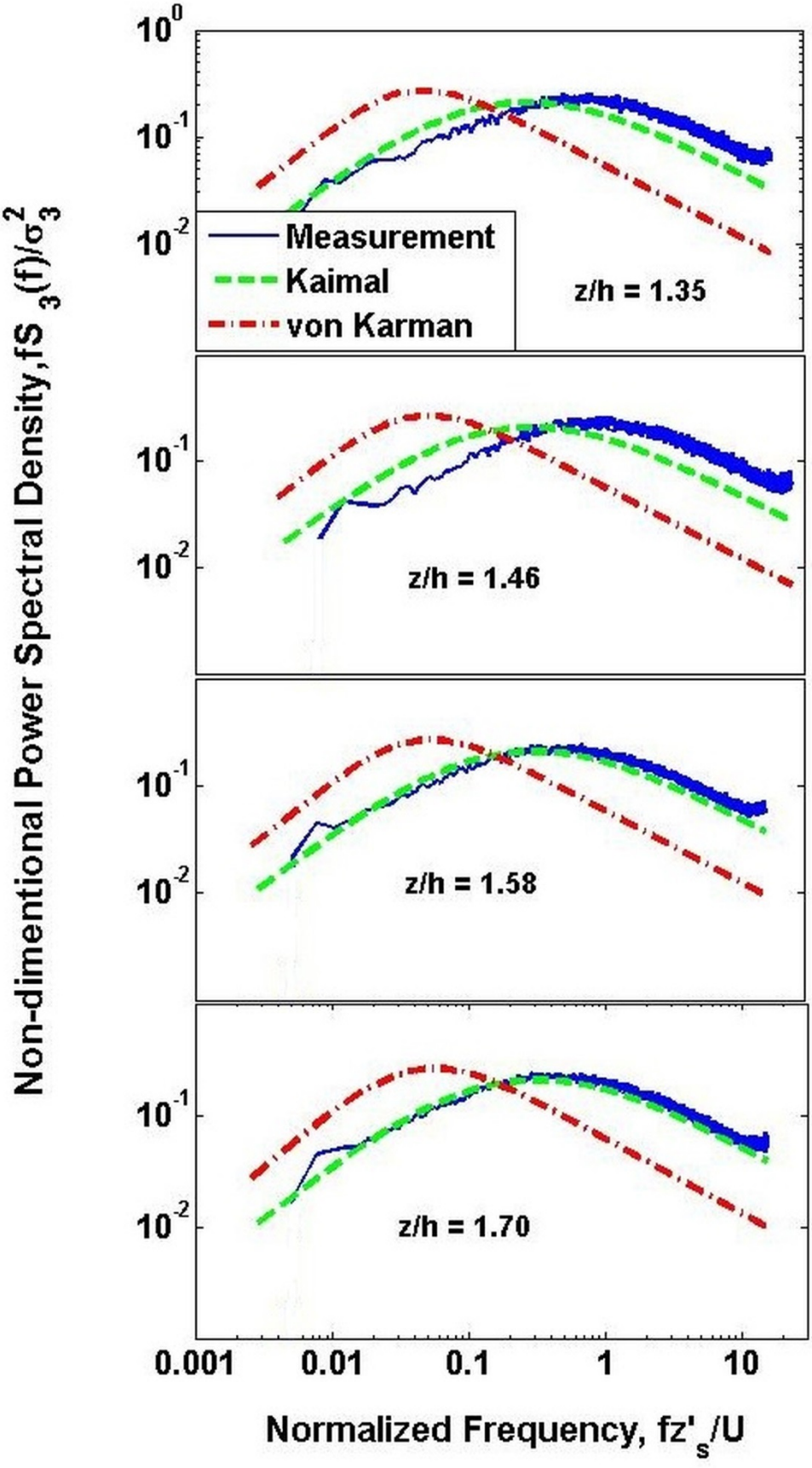

Figure 4c.Non-dimensional turbulence power spectral density of the **vertical** wind speed component for different heights above the rooftop of a warehouse in neutral atmospheric conditions.

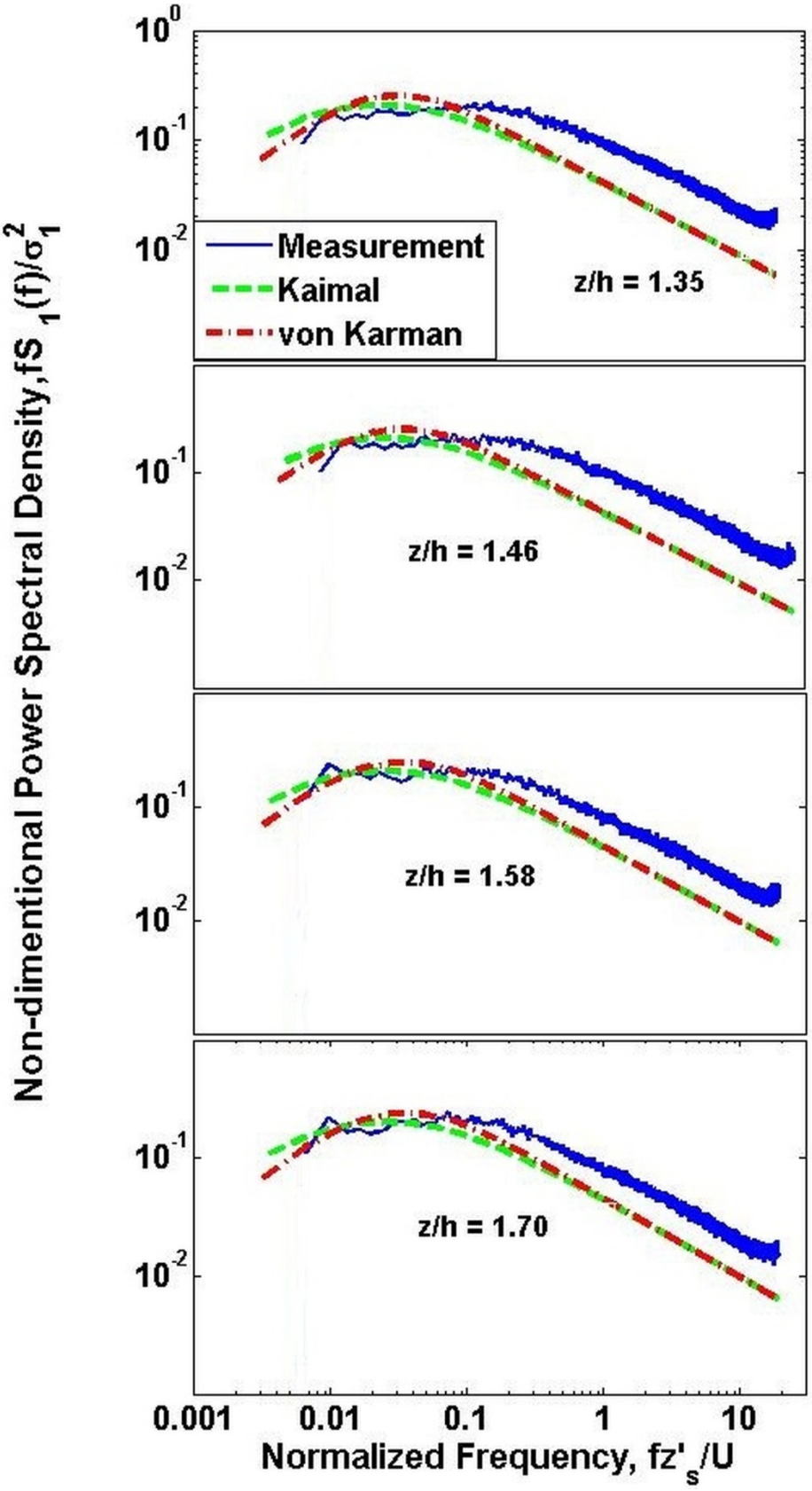

Figure 5a. Non-dimensional turbulence power spectral density of the **longitudinal** wind speed component for different heights above the rooftop of a warehouse in slightly unstable atmospheric conditions.

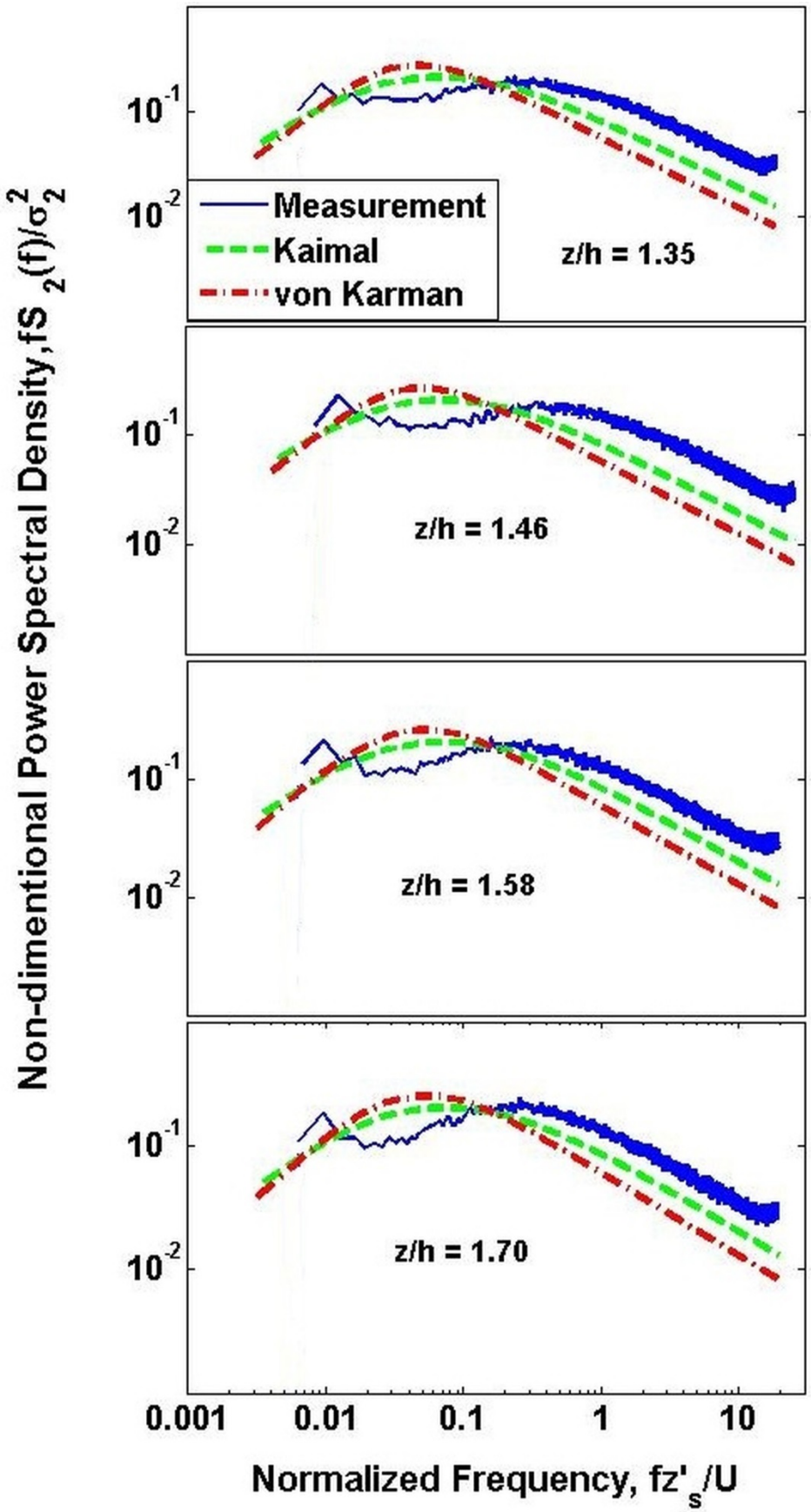

Figure 5b. Non-dimensional turbulence power spectral density of the **lateral** wind speed component for different heights above the rooftop of a warehouse in slightly unstable atmospheric conditions.

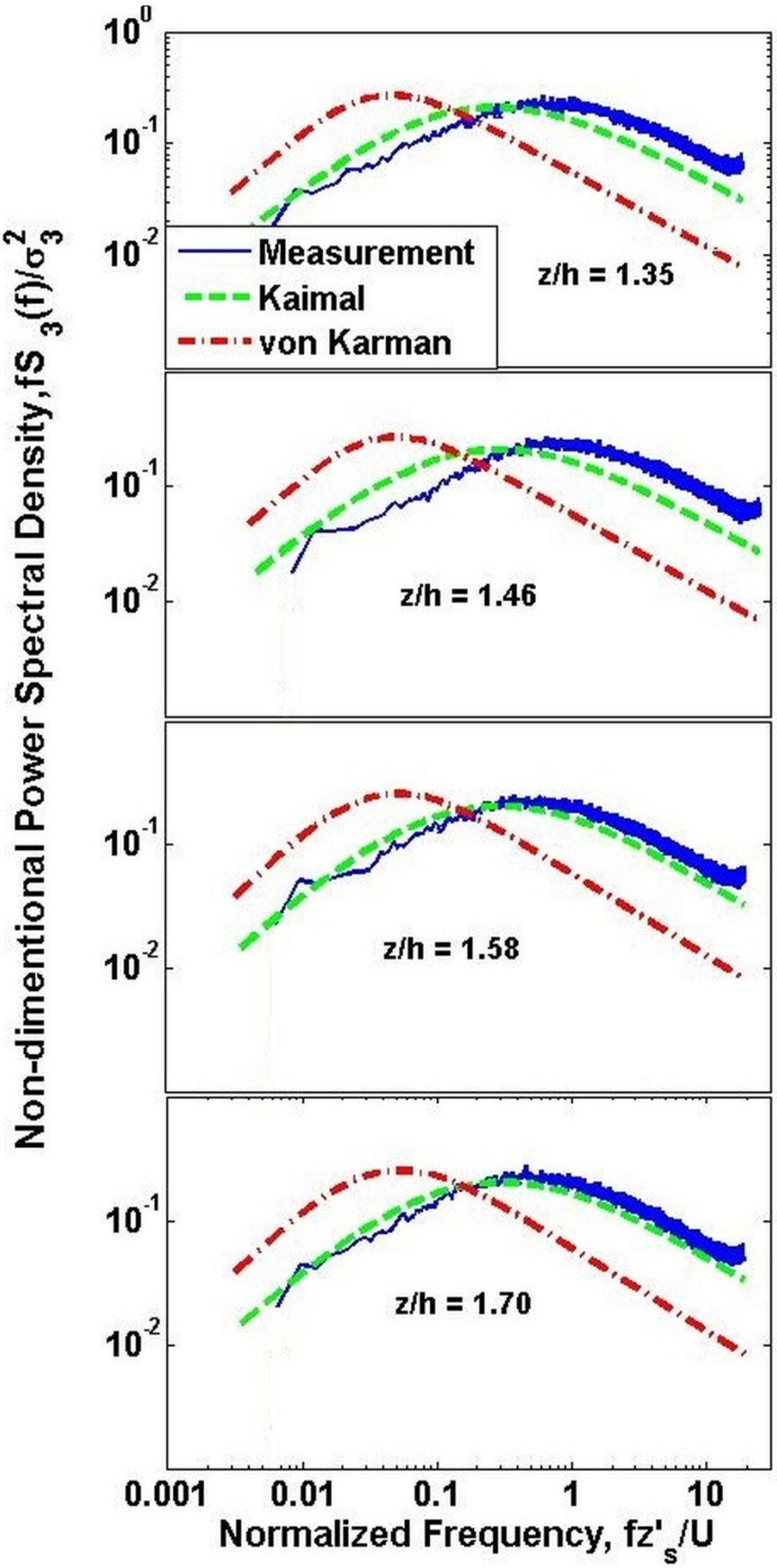

Figure 5c.Non-dimensional turbulence power spectral density of the **vertical** wind speed component for different heights above the rooftop of a warehouse in slightly unstable atmospheric conditions.

As is visually apparent from Figures 4 and 5, the longitudinal component of the spectra of the measured data is underestimated under both atmospheric conditions by both the von Karman and Kaimal models for normalized frequencies larger than around 0.1, although the Kaimal model appears closer to the measured values at lower frequencies. For the lateral component of Figures 4b and 5b, the models underestimate measured values at normalized frequencies above around 0.2 and overall the Kaimal model provides a better prediction. Figures 4b and 5b show what may be two peaks at low frequencies for the measured data. It is difficult to draw firm conclusions, however, and this behaviour may simply result from low numbers of data for the low-frequency part of the spectra. For the vertical component of Figure 4c, the calculated values from the von Karman model are markedly inaccurate whereas the values predicted by the Kaimal model underestimate the observed spectra close to the roof at normalized frequencies larger than around 0.5 but further from the rooftop the discrepancy becomes negligible.

The discrepancy between predicted and measured values on the rooftop is generally smaller for neutral atmospheric conditions, suggesting the models have higher accuracy under neutral atmospheric conditions. This is consistent with the formulation of the models since both von Karman and Kaimal turbulence models in the standard assume neutral atmospheric stability.

A more quantitative evaluation was performed through calculating the degree of misfit which is shown in Tables 2 and 3.

Table 2
Degree of misfit (d_{misfit}) assessing the misfit of the von Karman and Kaimal spectra to the measured spectra for different heights above the rooftop under neutral atmospheric conditions

Height	Wind Component	von Karman	Kaimal	No. of Records*
(z/*h* = 1.35)	Longitudinal	6.69	6.70	390
	Lateral	8.34	5.17	
	Vertical	13.57	3.82	
(z/h = 1.46)	Longitudinal	10.36	10.36	243
	Lateral	12.90	8.35	
	Vertical	20.41	6.56	
(z/h = 1.58)	Longitudinal	4.65	4.67	570
	Lateral	6.24	3.41	
	Vertical	10.42	1.85	
(z/h = 1.70)	Longitudinal	4.05	4.08	514
	Lateral	5.46	2.67	
	Vertical	9.73	1.30	

* Number of 10-minute records that were used in the averaging process.

Table 3
Degree of misfit (d_{misfit}) assessing the misfit of the von Karman and Kaimal spectra to the measured spectra for different heights above the rooftop under slightly unstable atmospheric conditions

Height	Wind Component	von Karman	Kaimal	No. of Records*
(z/*h* = 1.35)	Longitudinal	7.93	7.94	355
	Lateral	9.12	5.66	
	Vertical	14.77	4.28	
(z/h = 1.46)	Longitudinal	10.82	10.82	277
	Lateral	13.36	8.65	
	Vertical	21.24	6.91	
(z/h = 1.58)	Longitudinal	6.40	6.42	353
	Lateral	8.34	4.77	
	Vertical	13.69	2.83	
(z/h = 1.70)	Longitudinal	6.14	6.11	333
	Lateral	8.25	4.71	
	Vertical	13.15	2.40	

* Number of 10-minute records that were used in the averaging process.

The values of d_{misfit} in Tables 2 and 3 indicate that, the predicted results for both models have slightly better agreement with measurements under neutral atmospheric conditions. Generally, the values of d_{misfit} for the Kaimal model are clearly smaller compared to the equivalent values for the von Karman model in terms of lateral and vertical components, especially for the vertical component near to roof. This suggests the Kaimal spectra may provide more realistic predictions of the turbulence structure of lateral and vertical wind components in the built-environment. Such a result is hardly surprising as the von Karman model assumes isotropic turbulence and the conditions in the built environment are far from homogeneous. In terms of the turbulence spectra predicted for the longitudinal component, the values of d_{misfit} for both models are generally in agreement and the calculated values for d_{misfit} for both models decreased with increasing distance from the roof. Essentially, with increasing distance from the surface of the roof, the inhomogeneous structures from the underlying surface are averaged out and the turbulence becomes quasi-isotropic at least in the horizontal plane.

At high frequencies, whilst the von Karman and Kaimal models as outlined in IEC61400-2 can predict the trend, if not the magnitude, of longitudinal turbulence spectra in the built-environment, only the Kaimal model provides a reasonable estimate of the trend of turbulence spectra for the lateral and vertical components. The suggested form of the Kaimal model in IEC61400-2, however, cannot predict the magnitude of the turbulence spectra with a high degree of agreement compared to the actual turbulence conditions especially close to building surfaces.

5. Sensitivity Study

A sensitivity study is conducted to determine the sensitivity of the findings to choice of integral length scale in the model as well as to the selection of data from a particular wind direction.

5.1. Length scale

One likely reason for the inaccuracy of the Kaimal model in terms of predicting the magnitude of turbulence power spectra at the Port Kennedy rooftop site, is that the Kaimal

model as defined in IEC61400-2, assumes length scales of turbulence that are characteristic of open terrain [24]. The parameter of length scale represents the size of turbulent eddies [10] and in the built environment the scale of turbulence due to local inhomogeneties would be expected to be markedly different to the scales of turbulence in more uniform open terrain. Hence defining the length scale in terms of surface urban morphology may provide a more realistic estimation for use within the standard.

Figure 6 shows the impact of varying length scale on the Kaimal power spectral values model for longitudinal, lateral and vertical wind components at z/h = 1.46, under neutral atmospheric conditions. These graphs suggest that a more accurate prediction of the turbulence spectra at the Port Kennedy site could be obtained by persevering with the Kaimal model (since it predicts spectral trends reasonably well, particularly at higher frequencies) and using more appropriate length scales for the built environment in order to have agreement with the magnitude of measured spectral values. This is discussed further in Section 6.

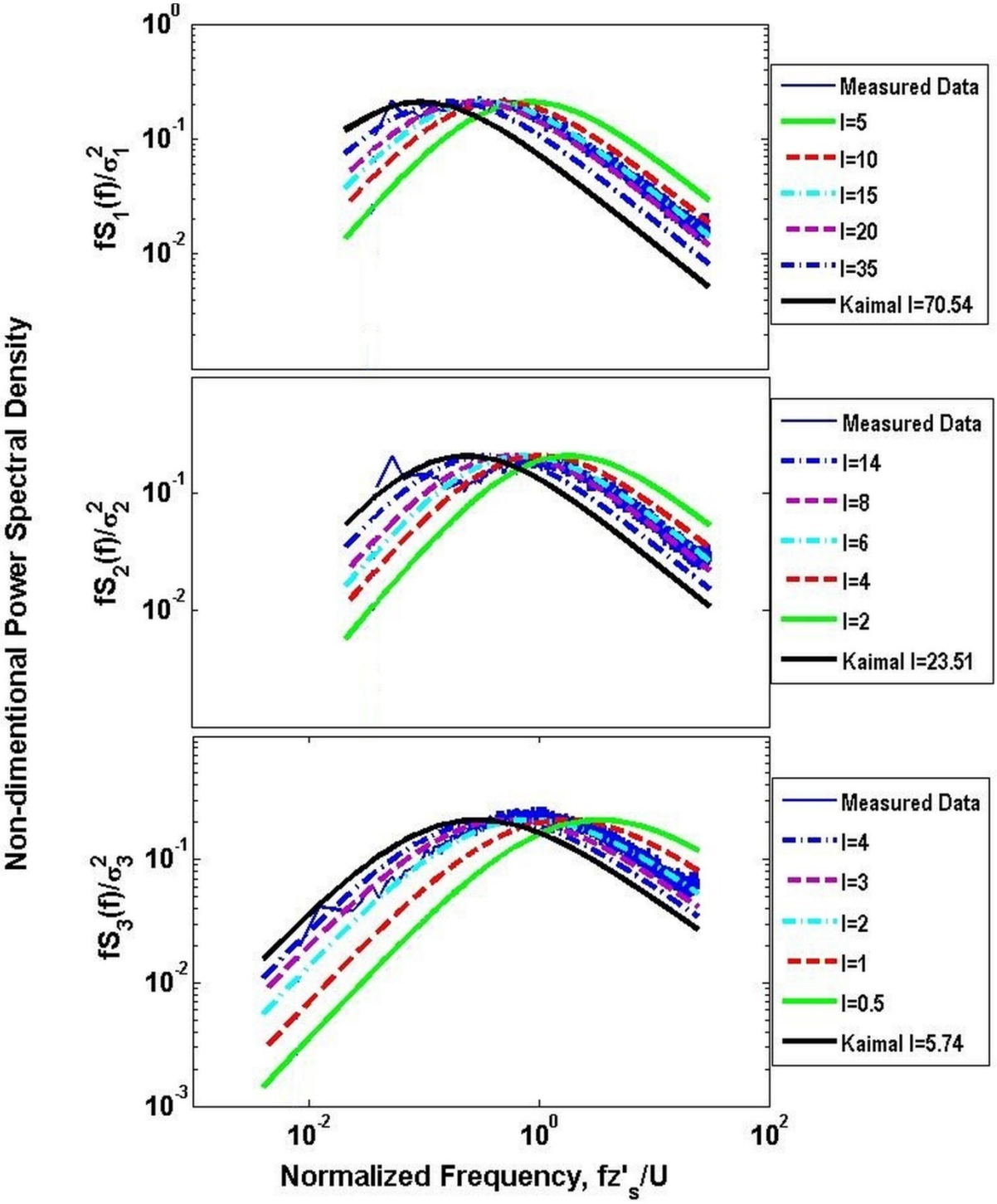

Figure 6.Non-dimensional turbulence power spectral density on the rooftop of a warehouse at z/h = 1.46 for different length scales in neutral atmospheric conditions.

5.2. Wind Direction

Since the models used in the standard are suitable for open terrain with no obstruction of the wind from any sector, the spectra equations (in this paper (7) to (10)) are independent of wind direction. The designer thus simulates 3D inflow to the turbine for the purpose of estimating turbine fatigue loads without any consideration of what direction the wind is coming from.

In the built environment, however, the turbulence spectra could be sensitive to wind direction. Figure 7 compares the average values of turbulence power spectral density for longitudinal, lateral and vertical wind components plotted against normalized frequency for south-east and south-west wind directions at z/h = 1.35, under neutral atmospheric conditions. The plots were the result of averaging 71 and 38 ten-minute recordings, for the south-east and south-west wind direction respectively.

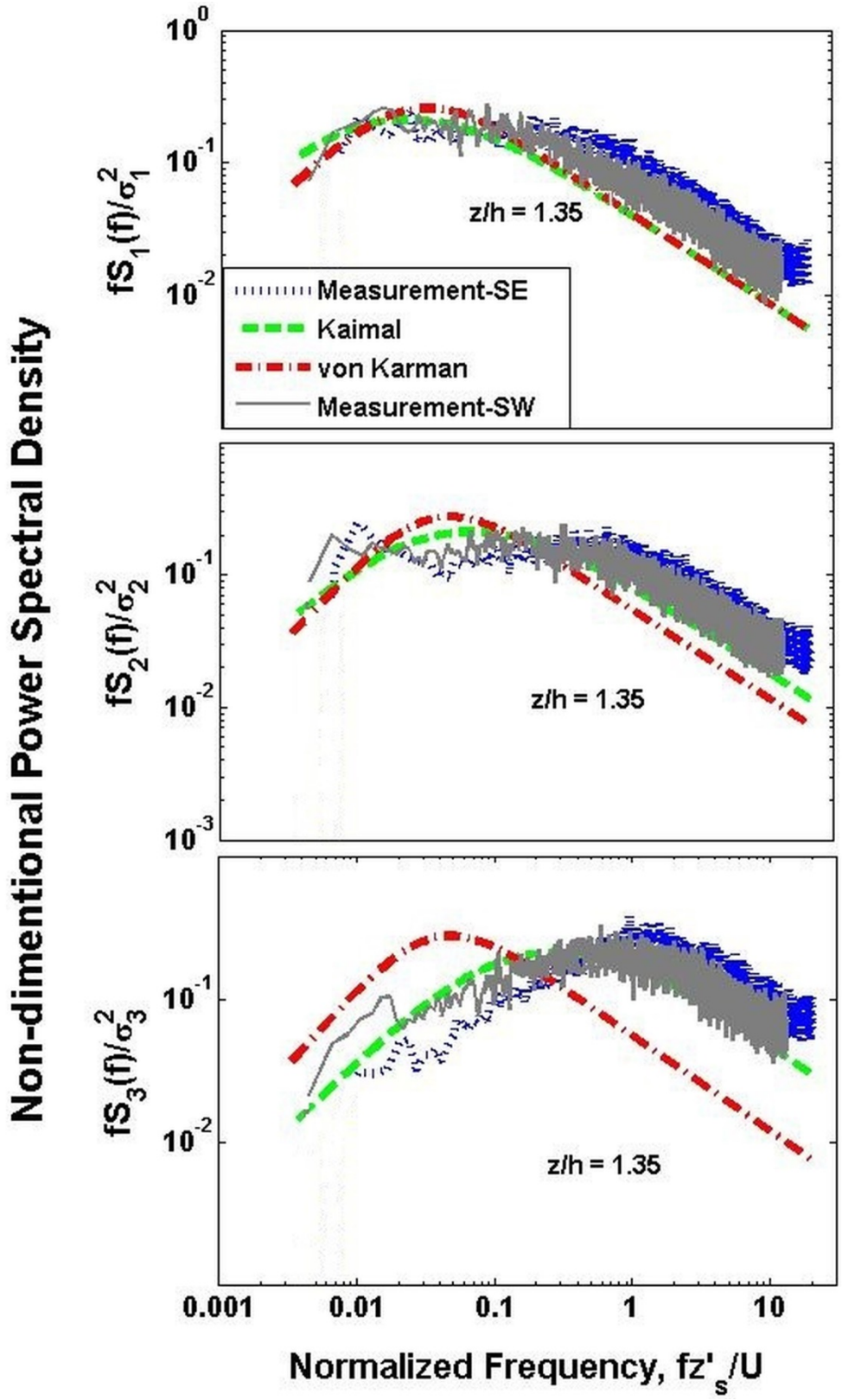

Figure 7.Non-dimensional turbulence power spectral density on the rooftop of a warehouse at z/h = 1.35 in neutral atmospheric conditions for south-east and south-west wind direction.

The graphs suggest, for all three wind components, that the Kaimal model is better at predicting the winds from the south west, even at lower frequencies. The most likely reason for this is that the terrain is more open from that sector and the Kaimal model does not perform as well for the wind from the south-east since the wind is coming over the southern end of the building before reaching the anemometer and turbines. Figure 7 suggests that sensitivity to the wind direction is an issue that a designer should investigate carefully in terms of the modelling of turbulence spectra on the rooftop of a building. A designer will need to make decisions based on how frequently winds come from different directions together with the turbine fatigue loads from those different directions.

6. Approach to modelling turbulence power spectra for a rooftop site

The results of this paper suggest that the Kaimal model is a good starting point to use in considering an approach to modelling turbulence power spectra for a rooftop site in the built environment. In terms of general trends in the power spectral density functions, both the von Karman and Kaimal spectra predict longitudinal turbulence spectra in the built-environment reasonably well particularly for high frequencies yet only the Kaimal model predicts the trends of the lateral and vertical wind components with any accuracy. In terms of the magnitude of the power spectra, the von Karman and Kaimal spectra under estimate the measured values for all wind components although the Kaimal spectra provides more realistic values than the von Karman spectra in terms of predicting the turbulence power spectra of lateral and vertical wind components in the built-environment.

The sensitivity study in Section 5, suggests that one important adaption of the Kaimal model to the built environment would be to choose a length scale that is suitable for the site. Currently the Kaimal model used in IEC61400-2 uses integral length scales as shown in Table 4, where the turbine is to be installed at a height z, less than 30 m (typical for a small wind turbine).

Table 4
Suggested integral length scales in the IEC61400-2 standard

	Velocity component index, k		
	1	2	3
Integral length scale, l_k	5.67z	1.89z	0.462z

A possible adaptive approach for the application of the Kaimal model in the built environment is proposed, where, the longitudinal integral length scale from Table 4 is substituted by a more appropriate length scale derived from Figure 6. Lateral and vertical integral length scales are then estimated using ratios of length scales appropriate for the built environment ($\frac{l_2}{l_1} = 0.5$ and $\frac{l_3}{l_1} = 0.15$) from studies by Christen et al. above the rooftop ($1<z/h<2$) of a street canyon [25].

Figures 9 and 10 show the results of comparing the new predictions from the suggested approach with the averaged values of the measured power spectra at the four different heights The figures shows that the adaptive approach suggested above results in more accurate

predictions by the Kaimal model over a large range of frequencies for all three wind components, in both atmospheric conditions, in terms of the model's application to sites in the built environment. Note that the model results at z/h = 1.46 show the worst discrepancies with the measurements compared to the other studied heights and this is likely to be due to the low number of data records at this height). Figures 9b and 10b show that the suggested approach can not accurately predict the low-frequency part of the lateral spectra. This lack of information, however, does not affect the conclusions of the present exercise because it concerns low frequencies, which Riziotis et al. (2000) [3] suggest are likely to be much smaller than the basic eigen-frequencies of a wind turbine and may not be important in terms of structural loading.

Tables 5 and 6 compare the values of d_{misfit} for the Kaimal model in the current IEC standard versus the results of the proposed approach. It is clear that the suggested approach for calculating length scale results in a much lower d_{misfit} than the current IEC standard approach for both atmospheric conditions.

In terms of the limitations of the study it must be noted that this approach to adapting the Kaimal model shows good agreement with measured data from just one rooftop site at Port Kennedy. Further data is required from other instrumented rooftop wind turbine installations to ascertain whether the approach can be generalized. In particular, further data is required on the ratios between lateral length scale value, vertical length scale value and longitudinal length scale value in the built environment. In order to provide uniform spectra for the built environment, one option may be to use the method, suggested by Coceal and Belcher, of deriving canopy parameters from urban morphological data and using them to estimate spectral length scales in the built environment [26].

In addition the measured data consisted of records over a period of 10 days taken at a specific time of the year. Further data is required from Port Kennedy in order to conduct an analysis of the effect of wind direction on turbulence spectra with a view to incorporating changes of spectra with wind direction into the adaptive approach. Finally, although there are five SWTs on the roof of the Bunnings building, this study collects data from only one rooftop location corresponding to the position of the anemometer. The positions of the turbines on the building should be taken into account when considering the inflow to the wind turbines mounted on a rooftop. Computational Fluid Dynamics (CFD) lends itself to this kind of study to avoid the expense and complexity of multiple measurement locations and the authors have conducted some previous work in this area using CFD [27].

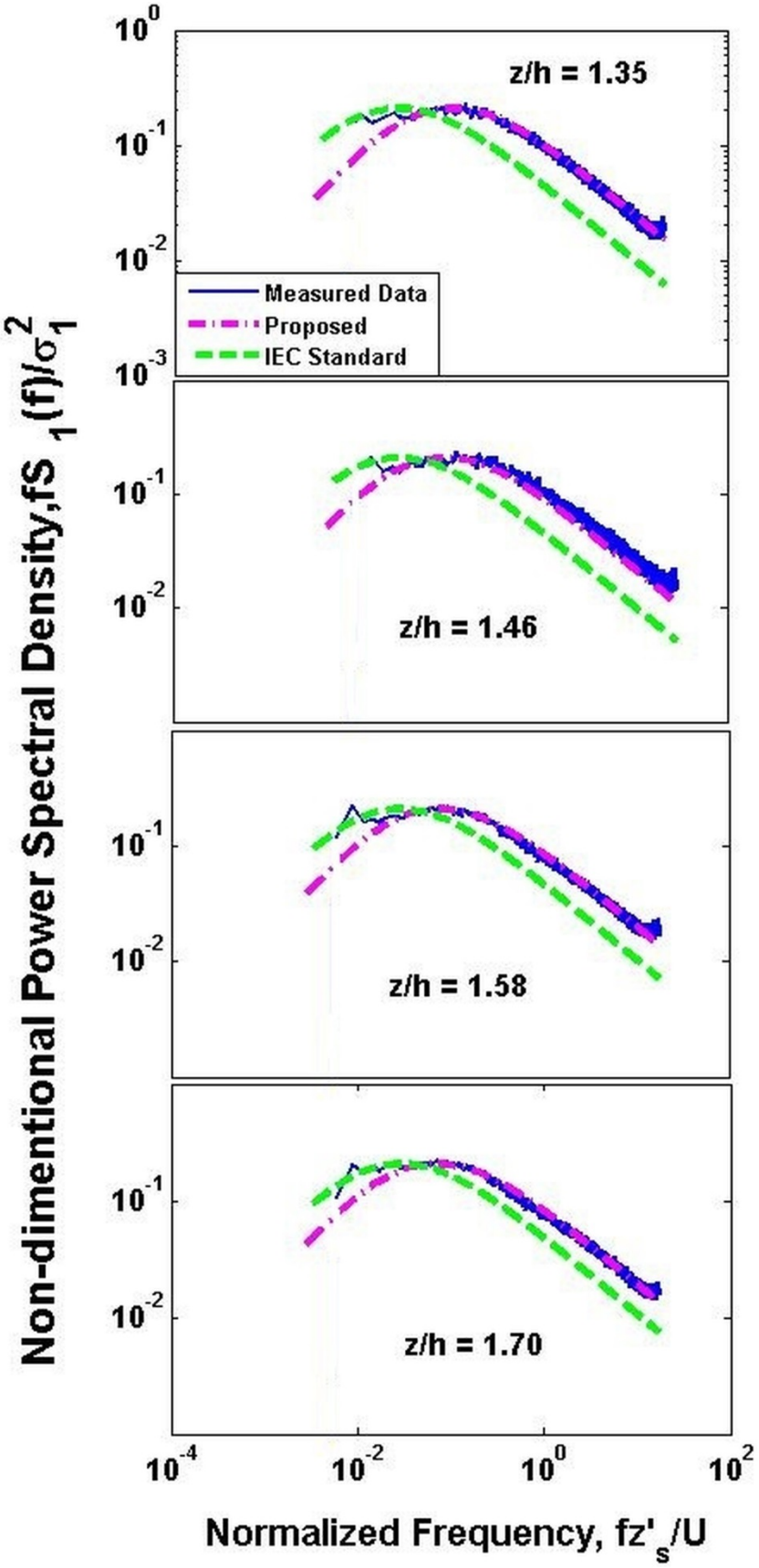

Figure 8a.Comparison of measured non-dimensional **longitudinal** turbulence power spectrum density and predicted values by Kaimal model via IEC standard approach and proposed approach for different heights above the rooftop of a warehouse in neutral atmospheric conditions.

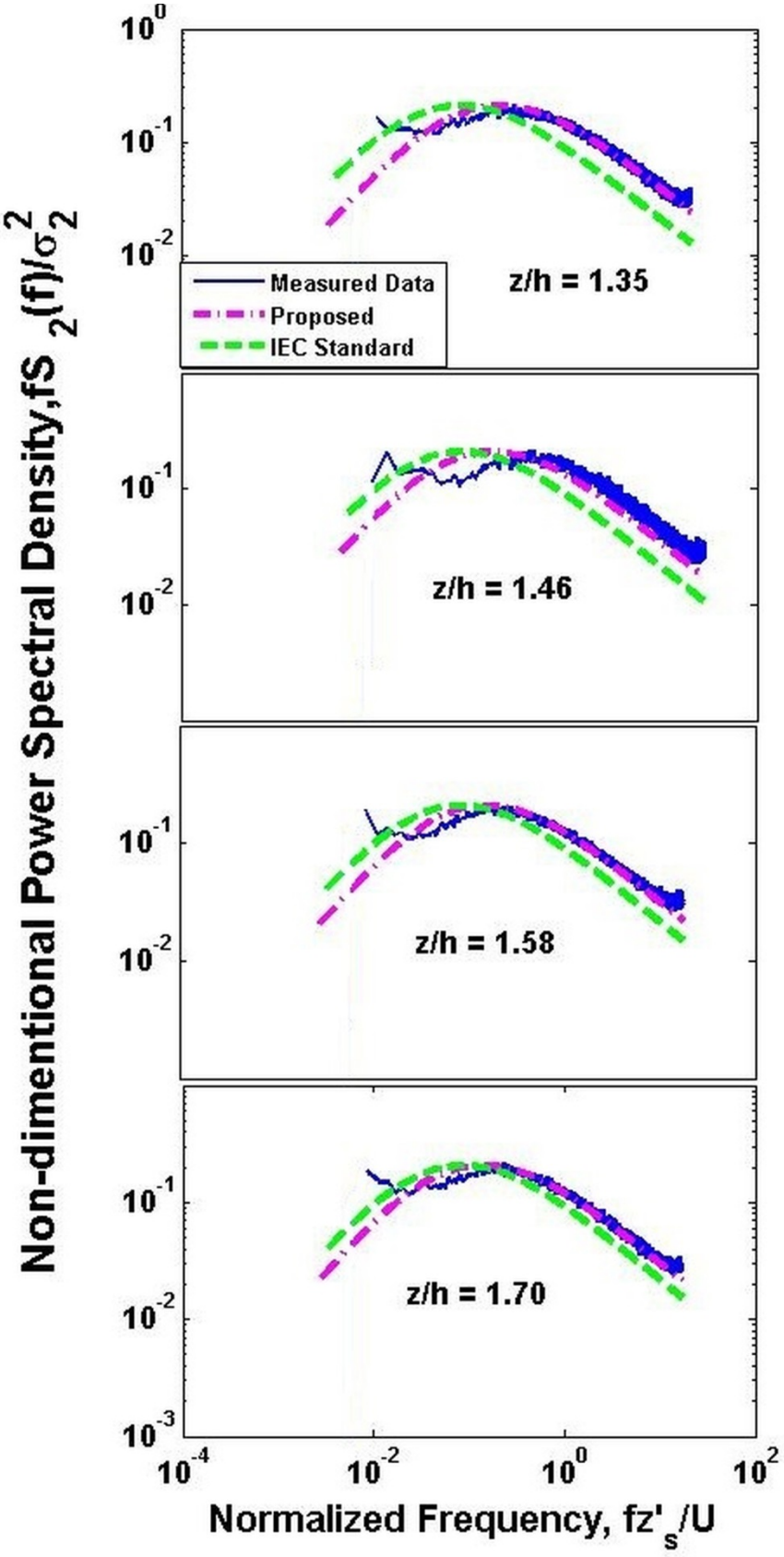

Figure 8b. Comparison of measured non-dimensional **lateral** turbulence power spectrum density and predicted values by Kaimal model via IEC standard approach and proposed approach for different heights above the rooftop of a warehouse in neutral atmospheric conditions.

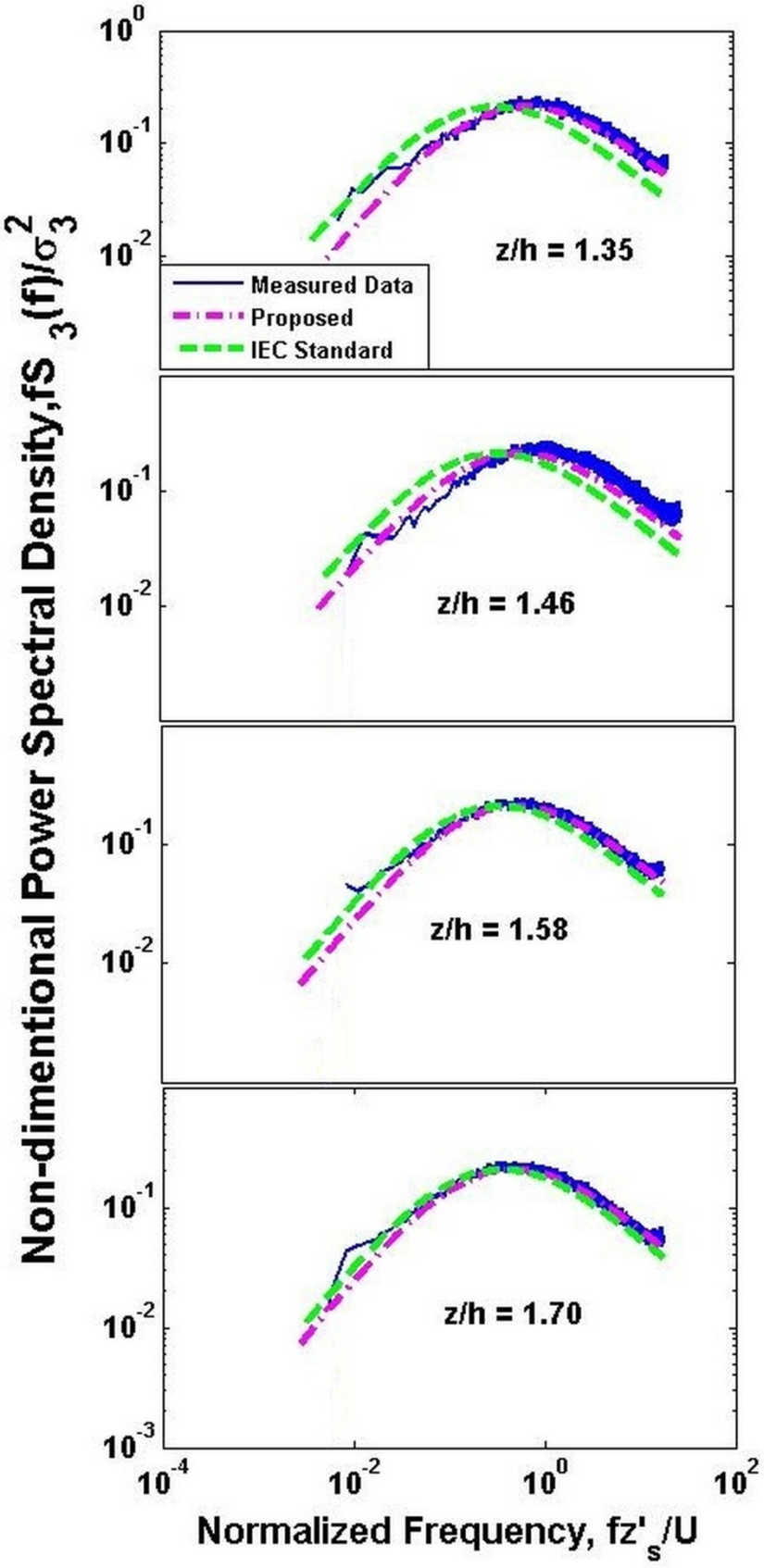

Figure 8c- Comparison of measured non-dimensional **vertical** turbulence power spectrum density and predicted values by Kaimal model via IEC standard approach and proposed approach for different heights above the rooftop of a warehouse in neutral atmospheric conditions.

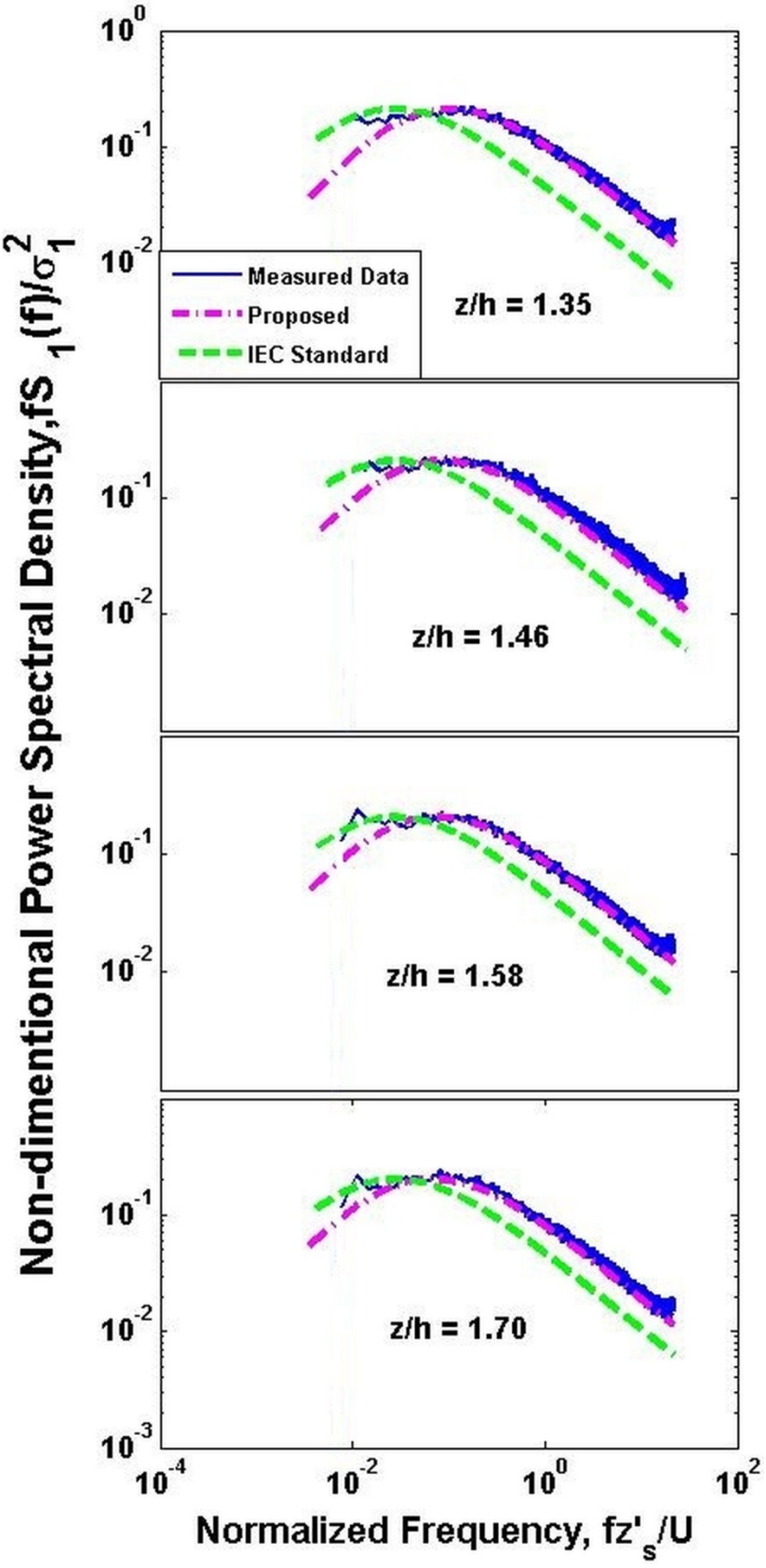

Figure 9a- Comparison of measured non-dimensional **longitudinal** turbulence power spectrum density and predicted values by Kaimal model via IEC standard approach and proposed approach for different heights above the rooftop of a warehouse in slightly unstable atmospheric conditions.

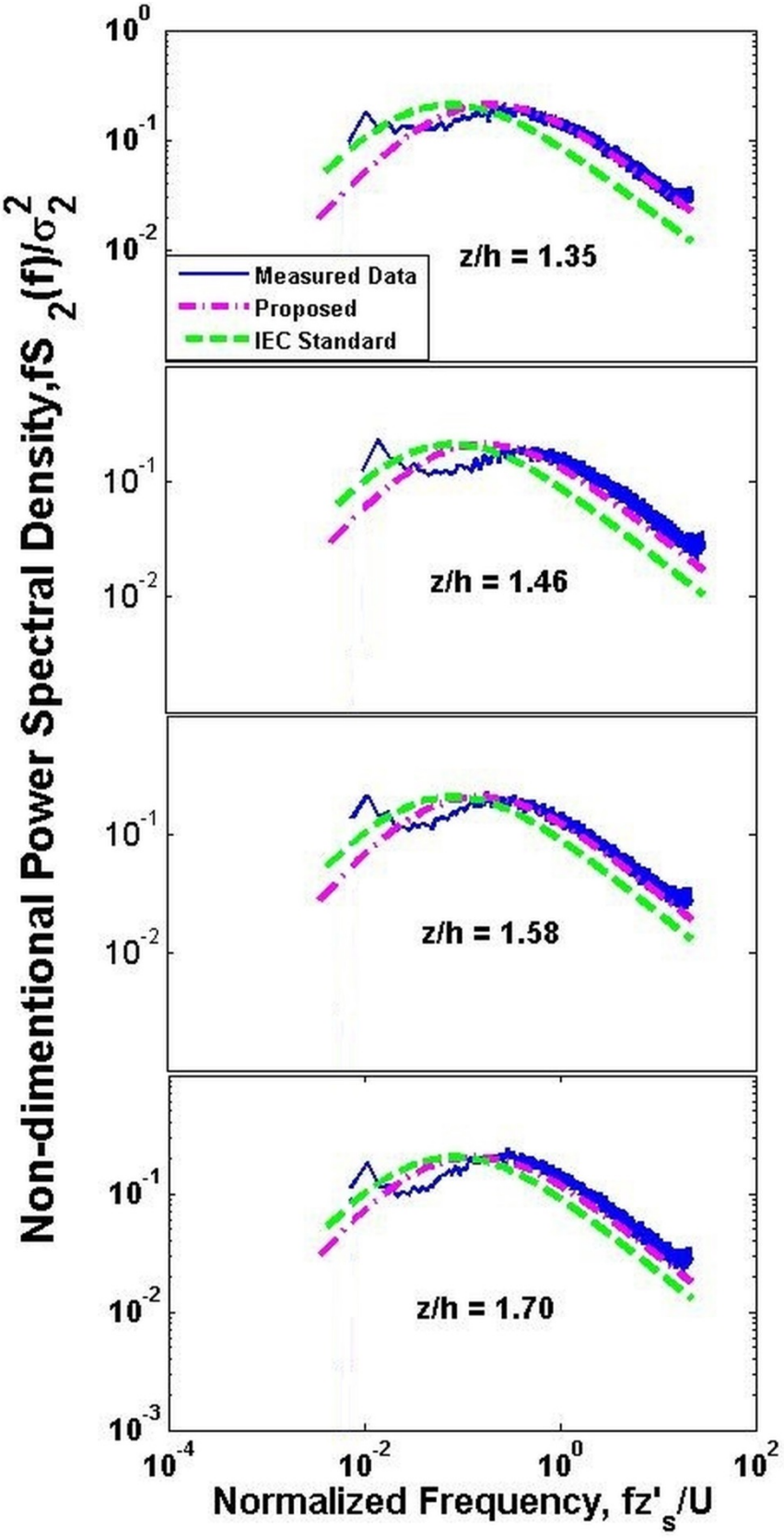

Figure 9b.Comparison of measured non-dimensional **lateral** turbulence power spectrum density and predicted values by Kaimal model via IEC standard approach and proposed approach for different heights above the rooftop of a warehouse in slightly unstable atmospheric conditions.

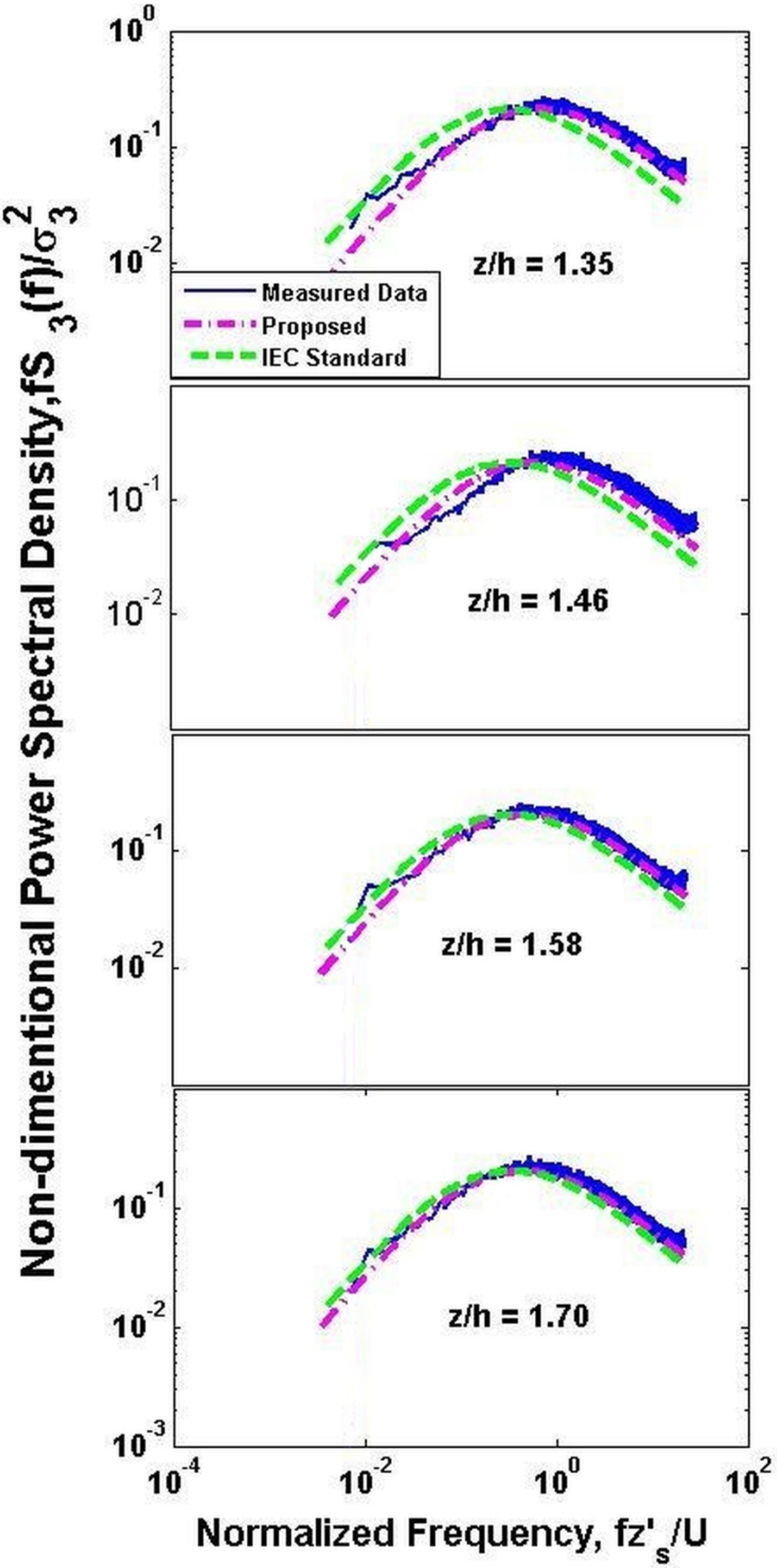

Figure 9c.Comparison of measured non-dimensional **vertical** turbulence power spectrum density and predicted values by Kaimal model via IEC standard approach and proposed approach for different heights above the rooftop of a warehouse in slightly unstable atmospheric conditions.

Table 5
Degree of misfit (d_{misfit}) assessing the misfit of Kaimal spectra via IEC standard approach and proposed approach to the measured spectra (neutral atmospheric condition)

Height	Wind Component	Kaimal IEC Standard	Kaimal Proposed	No. of Records*
(z/*h* = 1.35)	Longitudinal	6.70	0.23	390
	Lateral	5.17	0.37	
	Vertical	3.82	0.35	
(z/h = 1.46)	Longitudinal	10.36	1.36	243
	Lateral	8.35	1.86	
	Vertical	6.60	1.79	
(z/h = 1.58)	Longitudinal	4.67	0.34	570
	Lateral	3.41	0.57	
	Vertical	1.85	0.30	
(z/h = 1.70)	Longitudinal	4.08	0.32	514
	Lateral	2.68	0.46	
	Vertical	1.31	0.29	

* Number of 10-minute records that were used in the averaging process

Table 6
Degree of misfit (d_{misfit}) assessing the misfit of Kaimal spectra via IEC standard approach and proposed approach to the measured spectra (slightly unstable atmospheric condition)

Height	Wind Component	Kaimal IEC Standard	Kaimal Proposed	No. of Records*
(z/*h* = 1.35)	Longitudinal	7.94	0.42	355
	Lateral	5.66	0.43	
	Vertical	4.27	0.42	
(z/h = 1.46)	Longitudinal	10.82	1.46	277
	Lateral	8.65	1.92	
	Vertical	6.91	1.89	
(z/h = 1.58)	Longitudinal	6.42	0.62	353
	Lateral	4.77	0.98	
	Vertical	2.83	0.60	
(z/h = 1.70)	Longitudinal	6.11	0.86	333
	Lateral	4.71	1.40	
	Vertical	2.34	0.71	

* Number of 10-minute records that were used in the averaging process

7. Conclusion

The current IEC61400-2 standard uses stochastic turbulence models adapted from the von Karman and Kaimal power spectra in order to simulate flow fields that are used to predict structural loading on small wind turbines. The suitability of these power spectra for simulating turbulence in the built environment for small rooftop wind turbines has been investigated by comparing the model spectra with measured data on the rooftop of Bunnings' warehouse at Port Kennedy in Western Australia. The power spectra of all three wind components in neutral and slightly unstable atmospheric conditions at four heights above the rooftop are considered. A degree of misfit function (d_{misfit}) was used to compare von Karman, Kaimal and measured power spectra, as an indicator of model suitability.

In the light of the limitations of this study noted above the following conclusions can be drawn:

The Kaimal spectra predicted the trends of all wind components better than the von Karman model. This was particularly true at high frequencies which evidence suggests are the important frequencies when it comes to fatigue loading on wind turbines.

The results from this paper suggest that there are some key parameters that influence the shape and scale of the turbulence power spectra over the rooftop of a building that need to be taken into account when considering the inflow of a SWT installed on the roof. This paper has focussed on the influence of hub-height, atmospheric stability, turbulence length scales and wind direction. The models have greater agreement with measured data for higher hub-heights (further from the roofline) and in neutral atmospheric conditions. In the built environment, wind direction is important and will determine whether the inflow will be influenced by obstacles on the roof (including other SWTs), the building itself or by surrounding trees and buildings. Further research is required to study the effect of wind direction on turbulence spectra for Port Kennedy, involving collection of more data.

A sensitivity study with respect to length scale showed that prediction of spectra at high frequencies could be improved by using smaller length scales in the current model. This reduction in length scale is consistent with the cascading effect that obstacles in the built environment have on atmospheric turbulence whereby smaller eddies are generated. This is significant for small wind turbines as small eddies of the same scale as the order of the rotor diameter and the blade chord will have the greatest impact in terms of fatigue loading on the turbine rotor.

As an approach to modelling turbulence power spectra for a rooftop site in the built environment, an adapted Kaimal approach has been proposed that incorporates typical length scale ratios for that environment. The approach showed good agreement with measured data from the Port Kennedy site for all heights where there was sufficient measured data. The approach appears promising as a step forward on the path towards upgrading the existing standard with a dedicated design model for wind turbine manufacturers who intend their turbines to be used in highly turbulent sites such as the built environment. However, as stated previously, this study was limited to one rooftop site and further research is needed as to whether the approach will be appropriate for different rooftop sites. In order to propose an alternative expression for turbulent power spectra for rooftop sites that can be incorporated in the IEC61400-2 standard, a more comprehensive measurement program is required. Suggested future work includes a co-ordinated measurement campaign for various rooftop sites to accommodate changes in building geometry, turbine height, surrounding terrain and prevailing wind direction.

Acknowledgements

The authors would like to acknowledge Bunnings Group Pty. Ltd. for allowing Murdoch University researchers to conduct the wind monitoring campaign at the Port Kennedy warehouse. The authors are also indebted to Mr. Simon Glenister for maintaining the monitoring system and collecting data. Mr. Amir Bashirzadeh Tabrizi would like to thank Murdoch University for the award of a postgraduate scholarship. Dr. Jonathan Whale would like to thank the Hanse-Wissenschaftskolleg Institute of Advanced Study in Germany for the award of a research fellowship. Finally the authors would like to acknowledge the input of the anonymous referees in the peer-review process for their input in strengthening this paper.

References

[1] American Wind Energy Association, 2011 U.S. Small Wind Turbine Market Report, Year ending 2011.

[2] S. Mertens, Performance of an H-Darrieus in the skewed flow on a roof, *Journal of Solar Energy Engineering*, 125(2003) 433-440.

[3] V.A. Riziotis, S.G. Voutsinas, Fatigue loads on wind turbines of different control strategies operating in complex terrain, *J. Wind Eng. and Ind. Aerodyn.* , 85 (2000) 211-240.

[4] Wind-work by Paul Gipe, Available from: http://www.wind-works.org/cms/. [05/05/2014].

[5] A. Makkawi, A. Celik, T. Muneer, Evaluation of micro-mind turbine aerodynamics, wind speed sampling interval and its spatial variation, *Services Engineering Research and Technology*, 30 (2009) 7-14.

[6] E.E. Morfiadakis, G.L. Glinou, M.J. Koulouvari, The suitability of the von Karman spectrum for the structure of turbulence in a complex terrain wind farm, *J. Wind Eng. and Ind. Aerodyn.* , 62 (1996) 237-257.

[7] J.C. Kaimal, J.C. Wyngaard, Y. Yzumi, O.R. Cote, Spectral characteristics of surface layer turbulence, *Q. J. Roy Met. Soc*., 98 (1972) 563-589.

[8] J.C. Kaimal, J.C. Wyngaard, Y. Yzumi, O.R. Cote, Turbulence structure in the convective boundary layer, *J. Atmos. Sci*., 33 (1976) 2152-2169.

[9] ESDU, Characteristics of atmospheric turbulence near the ground, Part III: variations in space and time for strong winds (neutral atmosphere), ESDU Item Number 86010, October 1986. Available from: http://www.esdu.com/cgi-bin/ps.pl?sess=unlicensed_1141028041426byq&t =doc&p=esdu_86010e. [28/10/2014]

[10] B. S. Shiaua, Y. B. Chen, Observation on wind turbulence characteristics and velocity spectra near the ground at the coastal region, *J. Wind Eng and Ind.*, 90 (2002) 1671–1681.

[11] H.W. Tieleman, Universality of velocity spectra, *J. Wind Eng. and Ind. Aerodyn.*, 56 (1995) 55-69.

[12] IEC 61400-2, Wind turbines-Part2: design requirements for small wind turbines-Annex M, Third edition, International Electrotechnical Commission, Geneva, Switzerland, 2011.

[13] IEA wind task 27, Available from: http://www.ieawind.org/task_27_home_page.html. [05/05/2014].

[14] R.B. Stull, An introduction to boundary layer meteorology, Kluwer Academic Publishers, Vancouver, Canada, 1988.

[15] T.J. Lyons, W. D. Scott, Principles of air pollution meteorology, Belhaven Press, London, 1990.

[16] U. Högström, A.S. Smedman, Kompendium i atmosfärens grässkikt. Del1. Turbulensteori och skikten närmast marken. Uppsala university, Uppsala, Sweden, 1989.

[17] D. Golder, Relations among stability parameters in the surface layer, *Boundary Layer Meteorol*. 3 (1972) 47-58.

[18] J. F. Manwell, J. G. McGowan, A. L. Rogers, Wind energy explained: theory, design and application, First edition, John Wiley & Sons, Chichester ,2002.

[19] H. Wang, W.K. George, The integral scale in homogeneous isotropic turbulence, *Journal of Fluid Mechanics*, 459 (2002) 429-443.

[20] S. Maus, V. Dimri, Potential field power spectrum inversion for scaling geology, *Journal of Geophysical Research*, 100 (1995) 12605-12616.

[21] M.S. Hossain, Investigating whether the turbulence model from existing small wind turbine standards is valid for rooftop sites, MSc Dissertation, School of Engineering and Energy, Murdoch University, Perth, Australia, 2012.

[22] I. Troen, E. L. Petersen, European Wind Atlas, RisØ National Laboratory, Roskilde, Denmark, 1989.

[23] H.A. Panofsky, J.A. Dutton, Atmospheric turbulence, John Wiley & Sons, Ltd, New York, 1984

[24] Warwick Trials on building mounted turbines. Available from: http://www.bergey.com/technical/warwick-trials-of-building-mounted-wind-turbines. [05/05/2014].

[25] A. Christen, E. van Gorsel, R. Vogt, Coherent structures in urban roughness sublayer turbulence, *International Journal of Climatology*, 27 (2007) 1955-1968.

[26] O. Coceal, S. E. Belcher, Mean winds through an inhomogeneous urban canopy, *Boundary-Layer Meteorology*, 115(2005) 47–68.

[27] A. Bashirzadeh Tabrizi, J. Whale, T. Lyons, T. Urmee, Performance and safety of rooftop wind turbines: use of CFD to gain insight into inflow conditions. *Renewable Energy*, 67 (2014), 242-251.